

AMERICAN UNIVERSITY OF BEIRUT

DEREGULATED CAVEOLIN-1 AND HIC-5 EXPRESSION IN
MOUSE EMBRYO FIBROBLASTS LACKING A-TYPE LAMIN
AND HOMOZYGOUS FOR THE N195K MUTANT FORM

by
LARA ADNAN KAMAND

A thesis
submitted in partial fulfillment of the requirements
for the degree of Master of Science
to the Department of Biology
of the Faculty of Arts and Sciences
at the American University of Beirut

Beirut, Lebanon
March 2013

AMERICAN UNIVERSITY OF BEIRUT

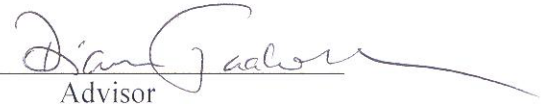
DEREGULATED CAVEOLIN-1 AND HIC-5 EXPRESSION IN
MOUSE EMBRYO FIBROBLASTS LACKING A-TYPE LAMIN
AND HOMOZYGOUS FOR THE N195K MUTANT FORM

By

LARA ADNAN KAMAND

Approved by:

Dr. Diana E. Jaalouk, Assistant Professor
Biology


Advisor

Dr. Rabih S. Talhouk, Professor
Biology


Member of Committee

Dr. Georges Nemer, Associate Professor
Biochemistry & Molecular Genetics


Member of Committee

Dr. Asad Zeidan, Assistant Professor
Anatomy, Cell Biology & Physiology


Member of Committee

Date of thesis defense: March, 7, 2013

AMERICAN UNIVERSITY OF BEIRUT

THESIS RELEASE FORM

I, Lara Adnan Kamand

- Authorize the American University of Beirut to supply copies of my thesis to libraries or individuals upon request.
- Do not authorize the American University of Beirut to supply copies of my thesis to libraries or individuals for a period of two years starting with the date of the thesis defense.

Signature

Date

ACKNOWLEDGEMENTS

“Now this is not the end. It is not even the beginning of the end. But it is perhaps, the end of the beginning”

Winston Churchill

When I first got enrolled in the MSc program, little did I know that it would turn out to be the most enriching experience ever, and I don't mean that at the academic level. But then again, life's most cherished moments are those that hit us unexpectedly, it is those moments that we learn from the most, value the most and carry with us in the years to come.

As this journey of mine is coming to an end, I feel great and looking forward eagerly for my next step as ambiguous as it may seem at the present moment, but at the same time, this means that I will be leaving behind people that have been in my life long enough to affect and change me.

Dr Diana, thank you, not for being the adviser you are and not for being the scientist you are but thank you for being the person you are. The past two years were anything but easy, yet we managed to survive the difficulties together. Now that it's over, I look back and I know for sure that I won't be the person that I was two years ago, I have changed, I have grown, I have matured and a lot of which, I owe to you.

Drs. Talhouk, Zeidan and Nemer. Thank you for agreeing to serve as members on my committee, your efforts are much appreciated.

To my parents, you have been by my side long enough to know that this is neither the first nor the last time that I will need you by my side. The ship might drift away and try to sail in the deepest waters once in a while, but no matter where it goes, it will always long to return to shore to safety to you. Lana, Dana, and Rasha you girls are the best, you are and always will be my rock. Scarfy, my dog, you have been a great support, seeing you was enough to make me forget the bad times that I went through.

Hind, Lori and Tamara and Raed, I can't thank you enough for being there for me. At times of hardship you took care of me and supported me, and I know for a fact that I couldn't have made this far if it were not you guys.

Nebye, I know you are thousand miles away now, but your presence in my life during the past couple of months gave me strength to go on. I am sure that it would have never been the same without you. You have helped me move on when I almost gave up. Finally, as challenging as it was, I made it.

AN ABSTRACT OF THE THESIS OF

Lara Adnan Kamand for Master of Science
Major: Biology

Title: Deregulated Caveolin-1 and Hic-5 Expression in Mouse Embryo Fibroblasts Lacking A-Type Lamin and Homozygous for the N195K Mutant Form

Laminopathies are a group of genetic diseases which result from mutations or altered post translational processing of nuclear envelope (NE)/lamina proteins. Most of these disorders are caused by mutations in the *LMNA* gene which encodes for the NE proteins lamins A/C that anchor other NE proteins to the nuclear membrane. *LMNA* mutations are manifested as diverse pathologies affecting a wide range of tissues. To date, the molecular mechanisms underlying the phenotypic diversity in laminopathies have not been deciphered; in particular how mutations in a ubiquitously expressed gene lead to tissue specific phenotypes. Many hypotheses have been proposed of which two stood out namely the “structural hypothesis” and the “gene-regulation hypothesis”. We are interested in the latter theory that proposes that altered tissue-specific gene expression may underlie the development of different disease phenotypes. Mechanosensitive genes are of interest in this context since many laminopathies affect mechanically strained tissues. We hereby hypothesize that there is dual deregulation of the mechanosensitive genes *Cav-1* (encodes for caveolin-1) and *Hic-5* (encodes for hypoxia inducible clone 5) in muscular laminopathies including Emery-Dreifuss Muscular Dystrophy (EDMD) and Dilated Cardiomyopathy (DCM). The objective of this study is to probe the expression of *Cav-1* and *Hic-5* in mouse embryo fibroblast (MEF) cell lines derived from mice either lacking A-type lamin expression (exhibit an EDMD phenotype) or homozygous for the N195K mutant form (exhibit a DCM phenotype). Real-Time PCR quantification of *Cav-1* expression at baseline conditions showed a decrease in caveolin-1 α transcript expression in *Lmna*^{-/-} and in *Lmna*^{N195K/N195K} MEFs. However, immunofluorescence staining and Western Blot analysis showed no significant difference in caveolin-1 α protein expression in both cell lines in comparison to wild-type controls, but putative differences in caveolin-1 α secretion are yet to be examined. Moreover, we noted marked elevation in *Hic-5* transcriptional expression at baseline conditions in both mutant cell lines and the response to H₂O₂ suggests a differential pattern of oxidative stress - induced *Hic-5* expression in both cell lines in comparison to wild-type controls. Intriguingly, immunofluorescence staining data showed no significant difference in *Hic-5* protein expression between the different cell lines.

However, there seems to be a differential expression of Hic-5 isoforms in *Lmna*^{N195K/N195K} MEFs in comparison to *Lmna*^{-/-} and wild-type controls as shown by Western Blot analysis. Taken together, our data indicate that there is dual deregulation in Cav-1 and Hic-5 expression in MEF cells lacking A-type lamin expression or expressing the DCM – causing N195K mutation. Our future aims would be to investigate whether *Cav-1* and *Hic-5* expression is deregulated in striated muscle cell lines and in muscle tissue samples derived from *Lmna*^{-/-} and *Lmna*^{N195K/N195K} mice. We also aim to study the effect of mechanical stress on modulating isoform –specific expression of *Cav-1* and *Hic-5* in these samples to gain a better insight into their roles in disease progression and pathogenesis in a more relevant context.

| | |
|-----------------------------|------|
| CONTENTS | Page |
| ACKNOWLEDGMENTS | v |
| ABSTRACT | vi |
| LIST OF ILLUSTRATIONS | xii |
| LIST OF TABLES | xiv |

Chapter

| | |
|---|----|
| I. LITERATURE REVIEW | 1 |
| A. Nuclear lamins and lamina | 1 |
| 1. Structure..... | 1 |
| 2. Function | 3 |
| B. Laminopathies | 5 |
| 1. Overview | 5 |
| 2. Muscular Laminopathies | 9 |
| a. Emery Driefuss muscular dystrophy | 9 |
| b. Dilated Cardiomyopathy | 11 |
| C. Caveolae and Caveolins | 13 |
| 1. Overview | 13 |
| 2. Caveolin-1 | 15 |
| 3. Caveolin-1 in mechanotransduction..... | 16 |
| 4. Caveolin-1 knockout and mutant mouse models..... | 17 |

| | |
|--|----|
| D. Hic-5 | 19 |
| 1. Overview..... | 19 |
| 2. Hic-5 in mechanotransduction | 21 |
| 3. Hic-5 ectopic expression and knockout mouse models | 22 |
| E. Laminopathies and oxidative stress | 23 |
| F. Gap in Knowledge, Rationale, and Hypothesis..... | 25 |
| G. Objective of the Study and Specific Aims | 27 |
| | |
| II. MATERIALS AND METHODS | 30 |
| | |
| A. Cell Culture | 30 |
| 1. <i>Lmna</i> MEFs (<i>Lmna</i> ^{+/+})..... | 31 |
| 2. <i>Lmna</i> null MEFs (<i>Lmna</i> ^{-/-}) | 30 |
| 3. <i>Lmna</i> ^{N195K/N195K} MEFs | 31 |
| B. RNA Extraction..... | 31 |
| C. Reverse transcription | 32 |
| D. Real-Time PCR | 33 |
| E. SDS page Western blot | 35 |
| 1. Protein extraction | 35 |
| 2. Protein quantification | 35 |
| 3. SDS-PAGE, preparing & running the gel | 36 |
| 4. Protein transfer gel to blot | 37 |
| 5. Western Blot, blocking, washing steps, antibody incubations | 38 |
| 6. Developing the western blot | 38 |
| 7. Striping the membrane with a different antibody | 39 |
| F. Immunofluorescence | 39 |
| G. Microscopic imaging | 41 |

| | |
|--|-----------|
| H. Image J Analysis | 41 |
| I. Statistical Analysis | 41 |
| III. RESULTS..... | 42 |
| Aim 1. <i>Cav-1 and Hic-5</i> expression at the transcriptional level in mouse embryo fibroblasts (MEFs) derived from mouse models of muscular laminopathies in comparison to wild-type controls cultured <i>in vitro</i> under baseline conditions | 42 |
| 1.1 <i>Cav-1</i> alpha gene expression is down-regulated in <i>Lmna</i> ^{-/-} MEFs (Lamin A/C null) and in <i>Lmna</i> ^{N195K/N195K} MEFs in comparison to <i>Lmna</i> ^{+/+} MEFs controls..... | 42 |
| 1.2 <i>Hic-5</i> gene expression data suggests an up-regulation in <i>Lmna</i> ^{-/-} MEFs (Lamin A/C null) and in <i>Lmna</i> ^{N195K/N195K} MEFs in comparison to <i>Lmna</i> ^{+/+} MEFs wild-type controls | 44 |
| Aim 2. <i>Cav-1 and Hic-5</i> expression at the protein level in MEFs derived from mouse models of muscular laminopathies in comparison to wild-type controls cultured <i>in vitro</i> under baseline conditions | 45 |
| 2.1 Immunofluorescence staining of Cav-1 α shows no significant difference in protein expression levels in <i>Lmna</i> ^{-/-} and <i>Lmna</i> ^{N195K/N195K} MEFs compared to <i>Lmna</i> ^{+/+} wild-type control | 45 |
| 2.2 Immunofluorescence staining of Hic-5 indicates no significant difference in protein expression levels in <i>Lmna</i> ^{-/-} MEFs and in <i>Lmna</i> ^{N195K/N195K} MEFs compared to <i>Lmna</i> ^{+/+} MEFs (wild-type controls) | 47 |
| 2.3 Western Blot analysis of Cav-1 α shows no significant difference in steady state protein expression levels in <i>Lmna</i> ^{-/-} MEFs and in <i>Lmna</i> ^{N195K/N195K} MEFs in comparison to <i>Lmna</i> ^{+/+} MEFs (wild-type controls)..... | 51 |
| 2.4 Western Blot analysis of Hic-5 protein expression suggests a differential expression of Hic-5 isoforms in <i>Lmna</i> ^{N195K/N195K} MEFs in comparison to <i>Lmna</i> null MEFs (<i>Lmna</i> ^{-/-}) and <i>Lmna</i> ^{+/+} MEFs (wild-type controls) | 52 |

| | |
|--|----|
| Aim 3. Investigating the effect of oxidative stress on the expression profile of <i>Cav-1</i> and <i>Hic-5</i> in MEFs derived from mouse models of EDMD and DCM in comparison to wild-type control | 55 |
| 3.1 Optimization of <i>H₂O₂</i> Exposure Parameter..... | 55 |
| 3.2 The response of <i>Lmna</i> null (<i>Lmna</i> ^{-/-}) and <i>Lmna</i> ^{N195K/N195K} MEF cells to oxidative stress induced by hydrogen peroxide compared to WT cells suggests a differential gene expression pattern for <i>Hic-5</i> between the three cell line..... | 58 |
| | |
| IV. DISCUSSION..... | 64 |
| | |
| REFERENCES | 72 |

ILLUSTRATIONS

| Figure | Page |
|---|------|
| 1. Post translational processing of the carboxyl terminal of prelamins A, B1, B2 | 3 |
| 2. Schematic representation of some of the reported mutations in the <i>LMNA</i> gene and the resultant laminopathies | 7 |
| 3. Diagram summarizing the membrane organization of lipid rafts and caveolae..... | 14 |
| 4. Schematic illustration of <i>Hic-5</i> signaling in response to TGF- β stimulation | 21 |
| 5. Theories proposed to explain the underlying phenotypic diversity in laminopathies.... | 26 |
| 6. <i>Cav-1α</i> gene expression in <i>Lmna</i> ^{-/-} MEFs and <i>Lmna</i> ^{N195K/N195K} MEFs cells at baseline conditions..... | 43 |
| 7. <i>Hic-5</i> gene expression in <i>Lmna</i> ^{-/-} and in <i>Lmna</i> ^{N195K/N195K} MEF cells quantified at base-line conditions..... | 45 |
| 8. Semi-quantitative assessment of the relative fluorescence intensity of caveolin-1 α immunostaining in <i>Lmna</i> ^{-/-} and in <i>Lmna</i> ^{N195K/N195K} MEF cells in comparison to WT control MEF cells at base line conditions..... | 47 |
| 9. Semi-quantitative assessment of the relative fluorescence intensity of <i>Hic-5</i> immunostaining in <i>Lmna</i> ^{-/-} and in <i>Lmna</i> ^{N195K/N195K} MEF cells in comparison to WT control MEF cells at baseline conditions..... | 49 |
| 10. Representative images showing immunofluorescence staining of caveolin -1 α and <i>Hic-5</i> in MEF cells deficient in A-type lamins and in MEF cells expressing the N195K mutant form in comparison to MEF cells expressing WT Lamin A/C..... | 50 |
| 11. Western Blot analysis of Cav-1 α protein expression in <i>Lmna</i> ^{-/-} and in <i>Lmna</i> ^{N195K/N195K} MEF cells vs. control WT cells at baseline conditions..... | 52 |
| 12. Western blot analysis of <i>Hic-5</i> protein expression in <i>Lmna</i> ^{-/-} and in <i>Lmna</i> ^{N195K/N195K} MEF cells vs. control WT cells at baseline conditions..... | 54 |
| 13. <i>Hic-5</i> immediate – early transcript expression normalized to that of <i>18S</i> reference gene in <i>Lmna</i> WT MEF cells following exposure to 0.1 and 0.5 μ M of H ₂ O ₂ at 4 different time points..... | 60 |

| | |
|--|----|
| 14. <i>Hic-5</i> immediate – early transcript expression normalized to that of <i>18S</i> reference gene in <i>Lmna</i> null MEF cells following exposure to 0.1 and 0.5 μM of H_2O_2 at 4 different time points..... | 61 |
| 15. <i>Hic-5</i> immediate – early transcript expression normalized to that of <i>18S</i> reference gene in <i>Lmna</i> N195K mutant MEF cells following exposure to 0.1 and 0.5 μM of H_2O_2 at 4 different time points..... | 63 |

TABLES

| Table | pages |
|--|-------|
| 1. Laminopathies grouped into those affecting cardiac and skeletal tissue (muscular laminopathies), pathologies that affect connective tissue such as adipose and bone, and HGPS which is manifested in many tissues..... | 7 |
| 2. A list showing the sequences of the forward and the reverse primers that were used to quantify the transcriptional expression of the α isoform of <i>CAV-1</i> , <i>Hic-5</i> , and the <i>18S</i> reference gene by Real-Time PCR | 34 |
| 3. A summary of the experimental parameters and the cell morphology observations made of the <i>Lmna</i> ^{+/+} MEF cells in response to varying concentrations of H ₂ O ₂ after 2hr of exposure | 56 |
| 4. A summary of the experimental parameters and the cell morphology observations made of the <i>Lmna</i> ^{+/+} MEF cells in response to varying concentrations of H ₂ O ₂ after 4hr of exposure | 57 |
| 5. A summary of the experimental parameters and the cell morphology observations made of the <i>Lmna</i> ^{-/-} and the <i>Lmna</i> ^{N195K/N195K} MEF cells in response to varying concentrations of H ₂ O ₂ after 2hr of exposure..... | 58 |

CHAPTER I

LITERATURE REVIEW

A. Nuclear Lamina and Lamins

1. Structure

The nuclear lamina is a network of type V intermediate filaments underlying the inner nuclear membrane of the nuclear envelope. Lamins and lamin - associated proteins make up the nuclear lamina, the former constituting the major part of it (Butin-Israeli *et al.*, 2012). Genes encoding for lamins increase in number and complexity as we move from lower metazoan to higher ones. In *C.elegans*, for example, lamin is expressed from a single lamin gene (*lmn-1*) whereas the human genome encompasses three lamin genes. In mammals, nuclear lamins are of two types A-type lamins and B-type lamins. They differ in their biochemical properties, their localization during cell cycle and in their sequence homology. A-type lamins include lamins A, C, C2, and AΔ10, of which isoforms A and C are expressed more often. These are encoded by a single gene, the *LMNA* gene, which gives rise to various isoforms by alternative splicing (Machiels *et al.*, 1996). The expression pattern of A-type lamins differs than that of the B-type lamins in that the former ones are not expressed in embryonic cells; it is only during differentiation that their expression is detected (Puckelwartz *et al.*, 2011). B-type lamins on the other hand are expressed in all somatic cells where they play a role during cell division as well as during organogenesis. B-type lamins include laminB1 and lamin B2 that are encoded by separate genes *LMNB1* and *LMNB2* respectively. Mice that lack

a functional *LMNB1* gene do not survive (Freund *et al.*, 2012). *In vitro*, mouse embryonic fibroblasts from these mice undergo premature senescence.

Nuclear lamins are the only intermediate filaments present in the nucleus. They are one out of six subtypes of the IF super family. They differ from the cytoskeletal IF by having an additional 42 amino acid residues at the coil 1b. They share the common tripartite structure with other IF components having a long α -helical domain flanked by a globular amino-terminal (head) domain and a carboxy-terminal (tail) domain (Dittmer *et al.*, 2011). The carboxy-terminal domain has an Ig domain, a CAAX box (except for lamin C) and a nuclear localization signal that allows its translocation into the nucleus. Lamin A, B1 and B2 are subjected to posttranslational modification. Briefly, these modifications take place at the C terminus. It is a stepwise process starting with the farnesylation (addition of a farnesyl group) of the cysteine residue of -CAAX by farnesyltransferase (Figure 1). It is followed by the cleavage of the -AAX by an endoprotease. Then, by the action of methyl transferase, the terminal carboxylic group COOH is methylated. At this point, the process diverges where prelamin A is subjected to the action of metalloprotease Zmpste24/FACE that cleaves the 15 amino acid carboxyl terminal yielding the mature lamin A. This step is absent in the case of lamin B1 and B2, hence they remain farnesylated (Dechat *et al.*, 2010). In addition to the above mentioned modifications that are required to generate mature A- and B- type lamins, other modifications include sumoylation, ADP- ribosylation and glycosylation. Phosphorylation is also one type of posttranslational modification that regulates the assembly and disassembly of nuclear lamins during cell cycle. In fact, under the action of Cdk1 and PKC the nuclear lamina disassembles at the onset of mitosis. A-type and B-type lamins differ in their localization after the disassembly of the nuclear lamina. In

fact, A-type lamins become concentrated in the cytoplasm as opposed to a more nuclear membrane associated localization of B-type lamins (Stick *et al.*, 1988). This disassembly is reversed by the action of protein phosphatase 1a leading to the reassembly of the structure during telophase-G1 transition (Gerace *et al.*, 1980; Heald *et al.*, 1990). Lamins interact with one another at the central rod domain, which has characteristic heptads repeats, to form dimers. Dimers then associate in a head to tail manner to form polymers.

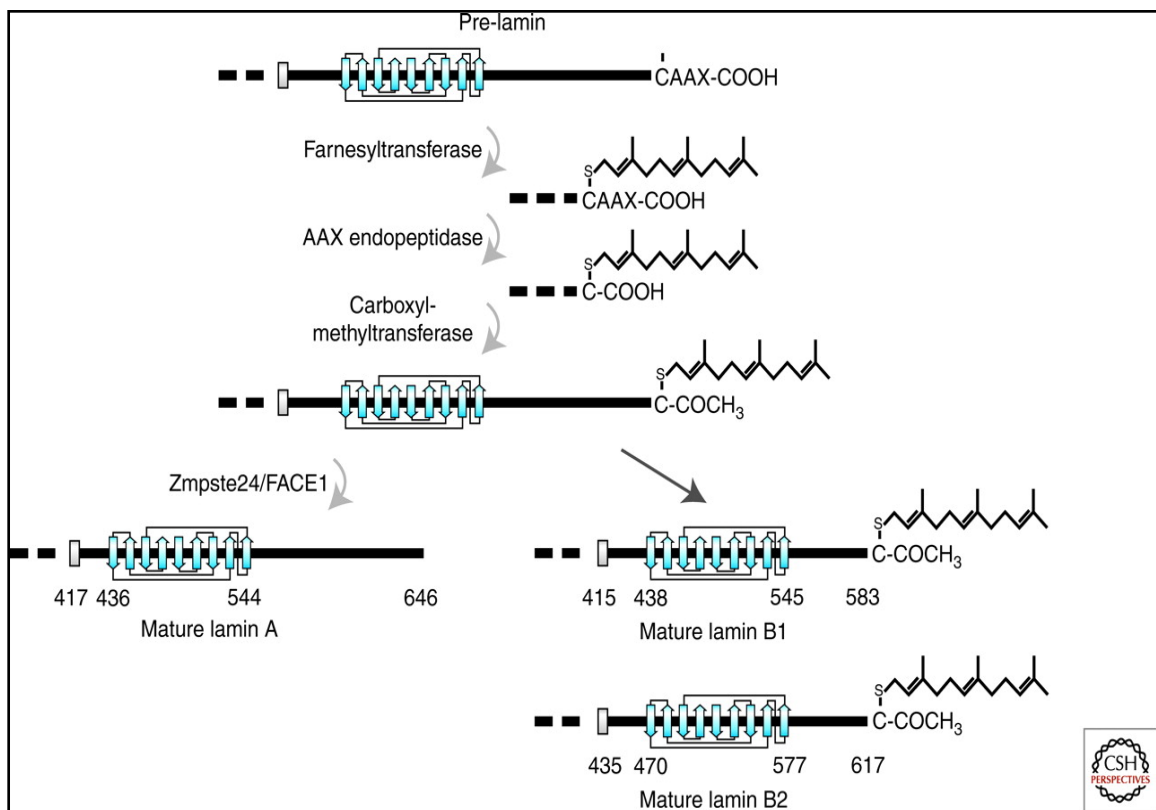


Figure 1: posttranslational processing of the carboxyl terminal of pre lamins A, B1 and B2 (image taken from Nuclear lamins, Dechat *et al.*, 2010).

2. Function

When the nuclear lamina was first discovered and by virtue of its position underneath the nuclear envelope, it was proposed that its function is largely to support

the nuclear envelope and to provide strength to it. However as more was being unveiled about this structure, more and more functions were attributed to it. Besides regulating the shape, size, and the mechanical properties of the nucleus; i.e. important in resisting nuclear deformation - which will be briefly discussed next - the nuclear lamina and the corresponding nuclear lamins also take part in chromatin organization and positioning, nuclear pore complex positioning, transcription and gene regulation, DNA synthesis and repair (Worman *et al.*, 2012).

Knowing that intermediate filaments of the cytoskeleton are involved in providing mechanical support to the whole cell, it was postulated that nuclear lamins function similarly in the nucleus. Subsequently, a number of studies have shown that cells lacking lamin A and C become more prone to mechanical stress and exhibit deformed nuclei (Broers *et al.*, 2004; Lammerding *et al.*, 2004). These cells also have impaired nucleoskeletal coupling which is needed for proper nuclear positioning, cell migration, cell polarization, and cytoskeletal organization (Méjat *et al.*, 2010; Folker *et al.*, 2011).

As mentioned above, the nuclear lamina is also involved in chromatin organization and consequently in gene regulation. The nuclear lamina represents an area where transcriptionally silent regions are preferentially situated. In addition, nuclear lamins harbor chromatin binding sites that mediate their interaction with chromatin. Such interactions can be direct or indirect; the latter being through histones or other proteins known to interact with lamins such as LAP2 alpha, lamin B receptor (LBR), emerin, MAN, etc. Nuclear lamins also interact with LADs which are transcriptionally repressive areas of the genome that mediate the specific interaction between the chromatin and the nuclear lamina. In addition, lamins as well as lamin-associated proteins interact with several transcription factors thereby controlling their

activity; these include cFos, protein retinoblastoma (pRb), ERK1/2, sterol regulatory element binding protein - 1 (SREBP-1), which is involved in transcription in adipocytes. Studies have shown that disruption in the nuclear lamina alters these mentioned interactions and disrupts the organization of chromatin leading to alteration in gene expression (Puckelwartz *et al.*, 2011; Maraldi *et al.*, 2011).

Nuclear lamins also act in DNA synthesis particularly during the elongation phase, where they are required for the assembly of the active elongation factors including PCNA and the large subunit of RFC complex. Studies have shown that the disruption of the nuclear lamina in such a way that the lamin proteins aggregate within the nucleoplasm led to a reduction in DNA replication (Spann *et al.*, 1997; Goldman *et al.*, 2002).

B. Laminopathies

1. Overview

Laminopathies are a group of genetic diseases which result from mutations or altered post translational processing of nuclear envelope (NE)/lamina proteins (Maraldi *et al.*, 2011). Most of these disorders are caused by mutations in the *LMNA* gene which encodes for lamins A/C that anchor the NE proteins to the nuclear membrane (Worman *et al.*, 2012). Over 400 mutations in the *LMNA* gene have been described so far. These mutations occur anywhere in the gene and are manifested as diverse pathologies affecting a wide range of tissues (Figure 2, Table 1). Laminopathies can be grouped into those affecting skeletal and cardiac muscles including autosomal dominant Emery-Dreifuss muscular dystrophy (EDMD) (Bonne *et al.*, 1999), X-linked Emery-Dreifuss muscular dystrophy (Bione *et al.*, 1994), limb-girdle muscular dystrophy type 1B

(Muchir *et al.*, 2000), dilated cardiomyopathy with conduction defects (DCM) (Fatkin *et al.*, 1999), and Charcot-Marie-Tooth disorder (De Sandre-Giovannoli *et al.*, 2002), and those affecting adipose tissues and bones including Dunnigan-type familial partial lipodystrophy (FPLD) (Cao *et al.*, 2000; Shackleton *et al.*, 2000), and mandibular-acral dysplasia (Novelli *et al.*, 2002). In addition, some rare laminopathies lead to premature aging and affect various tissue types; Hutchinson-Gilford Progeria syndrome (HGPS) and atypical Werner's syndrome fall into this category.

In muscular laminopathies, the mutations are dispersed throughout the gene; hence the polymerization of the nuclear lamina is defective. This causes a mechanically weak nuclear lamina in cells that are continuously subjected to mechanical stress. On the other hand, in case of laminopathies affecting adipose tissues, the mutations are concentrated in areas that affect the ability of lamin to interact with transcription factors such as SREBP-1 (Bertrand *et al.*, 2011).

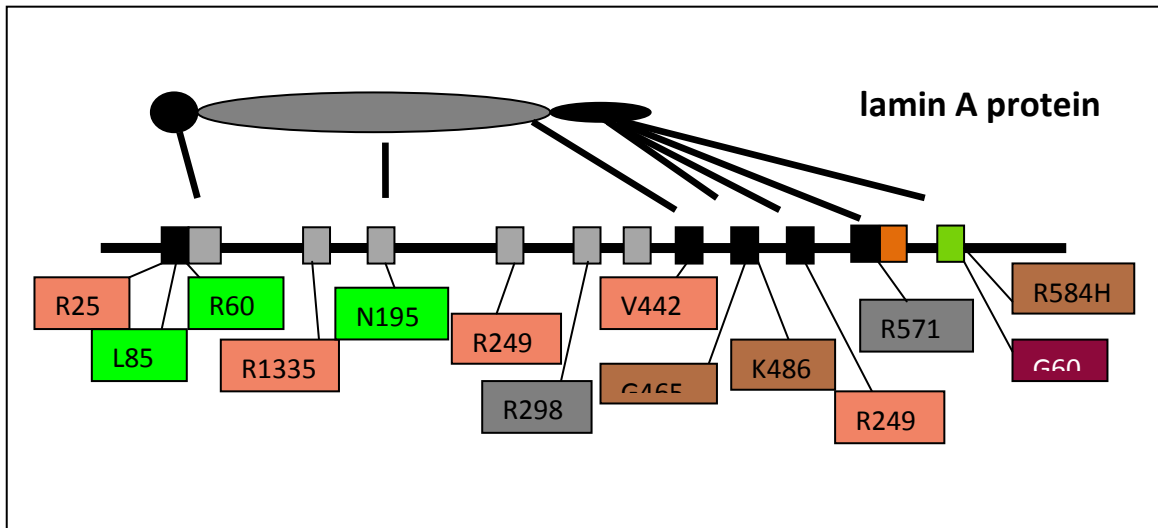


Figure 2: a schematic representation of some of the reported mutations in the *LMNA* gene and the resultant laminopathies. They are generally grouped into those affecting cardiac and skeletal tissue known as muscular laminopathies (green and orange), pathologies that affect connective tissue such as adipose and bone (grey and brown), and HGPS (red) which is manifested in multiple tissues.

Table 1: laminopathies are generally grouped into those affecting cardiac and skeletal tissue (muscular laminopathies), pathologies that affect connective tissue such as adipose and bone, and HGPS which is manifested in many tissues.

| Tissues affected | Laminopathy |
|-----------------------------|---|
| Cardiac and skeletal muscle | Dilated Cardiomyopathy (DCM) |
| | Limb Girdle Muscular Dystrophy |
| | Emery-Dreifuss Muscular Dystrophy (EDMD) |
| | Charcot-Marie-Tooth Disorder |
| Adipose and bone | Familial Partial Lipodystrophy (FPLD) |
| | Mandibular Acral Dysplasia |
| Multiple tissues | Hutchinson-Gilford Progeria Syndrome (HGPS) |

There are a number of lamin A/C-binding proteins implicated in laminopathies including lamin B2, nuclear envelope proteins such as MAN1, LBR, emerin, nesprins, the lamina-associated polypeptide LAP2 alpha, and the transcriptional regulator FHL1. These represent interacting partners with lamins either on the nucleoplasmic side, the nuclear envelope side, or both. LAP2 alpha, for instance, mediates the interaction of lamin A/C with the pRb/E2F pathway (Maraldi *et al.*, 2012). Accordingly, LAP2 alpha has been implicated in the proliferation and differentiation of muscle progenitor cells. Mutations in LAP2 alpha affecting the lamin A/C interacting domain lead to pathological heart condition similar to that resulting from mutations in the *LMNA* gene itself (Taylor *et al.*, 2005). In recent years, a number of tissue-specific pathways involved in the pathogenesis of laminopathies have been identified.

In familial partial lipodystrophies, the *LMNA* gene is found to be mutated exclusively in the C-terminal region restricted to codons 8 and 11 (Shackleton *et al.*, 2000). These mutations were found to disrupt the interaction between prelamin A, the unprocessed form of lamin A, and the sterol regulatory element binding protein 1 (SREBP-1). The latter is a transcription factor involved in adipogenesis and in cholesterol biosynthesis. It is synthesized as a precursor and remains associated with the endoplasmic reticulum where the decrease in the cholesterol level induces its intramembrane proteolysis and its translocation to the nucleus where it activates the transcription of genes involved in cholesterol metabolism including proliferator-activated receptor- γ (PPAR γ) (Heessen *et al.*, 2007). As such, prelamin A regulates the activity of SREBP-1 through sequestering it at the nuclear rim thus affecting its downstream signaling.

Hutchinson-Gilford Progeria syndrome is another disease caused by a mutation in the *LMNA* gene. The resultant progerin form of lamin A ($\Delta 50$) lacks 50 amino acids in which the endoproteolytic cleavage site by Zmpste 24 lies. This leads to incomplete processing of prelamin A which as a result remains attached to the membrane. In brief, TPR nuclear import is disrupted in HGPS. TPR is a nuclear pore complex associated protein; more specifically, it is a component at the nuclear side of the NPC. Along with its orthologues, TPR influences the NPC structure. In humans and drosophila, it is involved in spindle check points. It also affects mRNA export control, nuclear protein export, and takes part in silent telomeric chromatin organization and telomere length (David-Watine *et al.*, 2011). The nuclear import of TPR depends on the Ran gradient. In HGPS, the expression of progerin inhibits Ubc9 import that leads to a decrease in the levels of sumoylation by SUMO 2/3 and by the reduced function of RCC1, which is the chromatin-associated nucleotide exchange factor for Ran. Considering that both sumoylation by SUMO 2/3 and RCC1 levels affect the Ran gradient, TPR nuclear import is ultimately hindered leading to the gene expression changes described in HGPS (Joshua *et al.*, 2011).

2. Muscular Laminopathies

a. Emery - Driefuss Muscular Dystrophy

Emery - Driefuss Muscular Dystrophy (EDMD) is a disease caused by mutations in the *LMNA* or *EMD* genes coding for lamins A/C and emerin; another transmembrane protein of the inner nuclear membrane. In most cases, the disease is caused by mutations *in EMD* where it is inherited in an X-linked recessive manner (X-linked EDMD). However, when it is caused by mutations in the *LMNA* gene, the mode

of inheritance is mainly autosomal dominant (AD-EDMD) and in very rare cases it might be autosomal recessive (AR-EDMD).

EDMD is a progressive muscle wasting disorder affecting both skeletal and cardiac muscles and is characterized by early joint deformities called contractures affecting the Achilles tendons spine and elbows. It is also associated by cardiac conduction defects that result from abnormalities in the electrical signal controlling the heartbeat. Patients die of sudden heart block or develop progressive cardiac failure (Bonne *et al.*, 2001; Puckelwartz *et al.*, 2011).

To date, much is known about the genes and proteins that cause EDMD, but little is known about its pathogenesis. To this end, mouse models were designed to aid in understanding the role of lamin A/C and emerin in the development of EDMD. The first model of the disease was an *Lmna* knockout model (Sullivan *et al.*, 1999) where the post natal growth of mice was affected and the nuclear envelop structure was altered including a mis-localization of emerin protein. In EMD null mice, pathways pertaining to muscle regeneration were also affected. In fact, both MyoD and Rb1 gene regulated pathways were altered ultimately leading to delay or block in the myoblast/myotube transition during differentiation (Melcon *et al.*, 2006).

Studies also show that ERK1/2 signaling pathways are heavily implicated in development of cardiomyopathy. Activation of MAPK in turn leads to activation of several downstream genes encoding for transcriptional factors that regulate the expression of genes involved in cardiomyofiber and sarcomere organization (Thorburn *et al.*, 1995). In that regard, the hearts of *EMD* null mice showed activation of ERK branch of MAPK pathway. Moreover, hearts from mice expressing

the *Lmna*^{H22P/H22P} mutation that leads to EDMD also showed an over activation of MAPK pathway.

Interestingly, caveolin-1 and caveolin-3 knockout mice also show an over activation in the MAPK pathway and suffer from cardiomyopathy (Cohen *et al.*, 2003; Woodman *et al.*, 2002) in what might serve as a link between caveolin-mediated signaling pathways and muscular laminopathies.

b. Dilated Cardiomyopathy

Dilated Cardiomyopathy (DCM) is a myocardial disorder defined by ventricular chamber enlargement and systolic dysfunction. It can result in progressive heart failure, arrhythmias, thromboembolism, and premature death (Fatkin *et al.*, 2010). The causes behind such a disorder are diverse and in most cases they are unknown, hence referred to as idiopathic. In some cases, the damage of the myocardium could be due to infectious, toxic or metabolic agents. Viral infections such as those of Coxsackie B virus and other enteroviruses can also cause damage to the myocardium ultimately leading to DCM. Of relevance to us is DCM caused by genetic mutations. In most cases, the disease is transmitted in an autosomal dominant manner, where around 26 genes were identified so far, most of which encode for structural component of the heart muscle, thus hinting to the involvement of impaired force generation, sensing and transmission. In addition, a dozen of other mutations affecting other aspects of the cardiac myocyte have been identified including those disturbing the nuclear structure, ion regulation and Ca²⁺ metabolism (Parvari *et al.*, 2012).

When the muscle contracts, it generates force that is transmitted along; however, in case of mutations in the dystrophin gene, for instance, which is responsible for anchoring muscle cells, the force transmission is hindered leading to DCM. In addition, a number of other genes involved in muscle cell anchorage have also been linked to DCM; these include laminin, metavinculin, a splice variant of vinculin, and dystrobrevin. Of importance to muscle contraction is the concentration of intracellular Ca^{2+} which is regulated by phospholamban protein, where it has been reported that mutation in *PLB* leading to the deletion of arginine 14 results in lethal hereditary Cardiomyopathy (Haghighi *et al.*, 2006). DCM is also caused by mutations that alter the function of the mitochondria. For example, mutations in Coenzyme Q10, a mobile lipophilic electron carrier located in the inner mitochondrial membrane leads to a multisystem disorder among which is DCM (Duncan *et al.*, 2009).

Finally, mutations in *LMNA* and *EMD* have also been reported to cause DCM. One example is the *Lmna*^{N195K/N195K} mutation. Mutant mice homozygous for the *Lmna-N195K* variation show signs of cardiomyopathy by the age of 9 weeks. Interestingly, they also show abnormal distribution for the gap junction protein connexin 40 responsible for impulse conduction. In addition, the expression pattern of some genes including the transcription factor HF1b/Sp4 is altered. Also, the response of cardiomyocytes in these mouse models to force conduction is altered possibly due to overall decreased ability of *Lmna*^{N195K/N195K} cells to institute an adequate stress response (Lammerding *et al.*, 2004). This clearly indicates that the affected tissues are subjected to mechanical stress and that their response to stress is mediated by lamin A/C protein which is greatly hindered in muscular laminopathies.

C. Caveolae and Caveolins

1. Overview of Caveolins

Caveolae are non-clathrin coated invaginations of the plasma membrane that are highly enriched with cholesterol and sphingolipids. The word caveolae refers to “small caves” with flask - shaped morphology. They have a diameter of 50-100 nm and are present in a wide range of tissues and cells including myocytes, fibroblasts, endothelial cells, epithelial cells and adipocytes. Caveolins are the primary components of caveolae. The caveolin gene family has three members in vertebrates namely *CAV1*, *CAV2*, and *CAV3* encoding for the proteins caveolin-1 (Cav-1), caveolin-2 (Cav-2), and caveolin-3 (Cav-3) respectively. At the protein level, vertebrates express four forms: Cav-1 α and Cav-1 β encoded by the same gene whereas Cav-2 and Cav-3 are encoded by two separate genes. Cav-1 α and Cav-1 β are generated by differential RNA splicing such that the β isoform lacks the first thirty three amino acids. Along with Cav-2, both Cav-1 isoforms are present in non-muscle cells, whereas myocytes express all four caveolins (Fang *et al.*, 2006). Cav-1 is a main component of the caveolae plasma membranes found in most cell types where it acts as scaffolding protein within caveolar membranes. Cav-1 and Cav-2 have similar expression patterns and seem to be co-expressed. On the other hand, the expression of Cav-3 is restricted to striated and smooth muscle cells. Cav-1 α , Cav-2, and Cav-3 possess a 33 amino acid hydrophobic domain that forms a hairpin loop inserted into the membrane where both their C-terminus and N-terminus face the cytosol (Boscher *et al.*, 2012). By virtue of its location in caveolae, Cav-1 plays a role in integrin signaling linking integrin subunits to the tyrosine kinase FYN; an initiating step in coupling integrins to the Ras-ERK pathway and in promoting cell cycle progression. Additionally, Cav-1 has been

implicated in a number of pathways including caveolar mediated endocytosis signaling, G-protein beta/gamma signaling cascades, cell adhesion tight junctions, and gap junctions, and cytoskeletal remodeling. It has also been shown to interact with multiple receptors including transforming growth factor beta (TGF β) receptor 1, and epidermal growth factor receptor (EGFR). Mutations in the *CAVI* gene have been associated with a number of diseases among which are muscular dystrophies (www.genecards.org/cgi-bin/carddisp.pl?gene=CAV1).

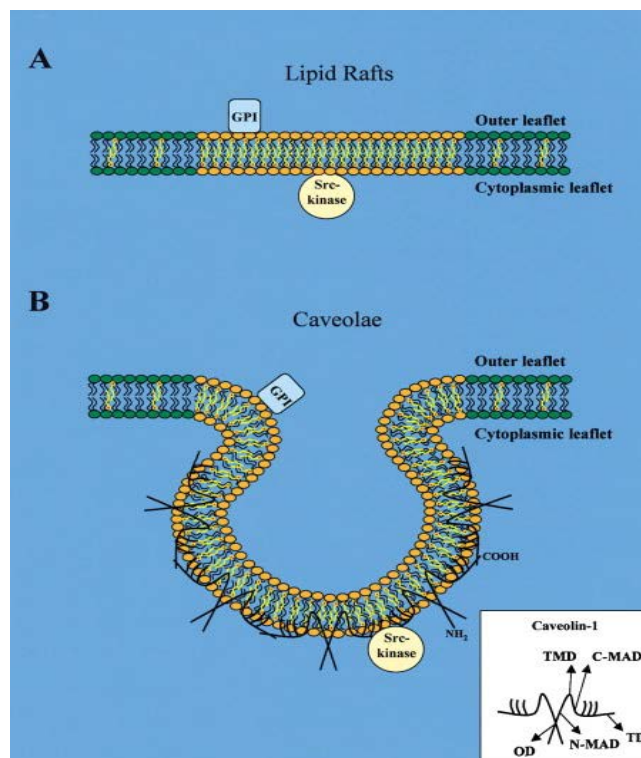


Figure 3: Diagram summarizing the membrane organization of lipid rafts and caveolae (Galbiati *et al.*, 2001).

2. Caveolin- 1

As mentioned above, *CAV-1* gene in vertebrates gives rise to two isoforms Cav-1 α and Cav-1 β . Early reports suggested that these two isoforms arise from the same mRNA by alternative translation, but it was later shown that they result from alternative splicing. In their study of embryogenesis in the zebra fish model, Fang *et al* demonstrated that these isoforms exhibit overlapping but distinct distribution (Fang *et al.*, 2006). It has been determined that the presence of both isoforms is required for proper caveolae formation, for cytoskeletal organization, and endothelium formation. Intriguingly, the two isoforms have non overlapping functions given that the defects caused by depletion of one of them are not rescued by the heterotypic isoforms. Expression wise, Cav-1 α is the only isoform expressed in intestinal epithelium suggesting its distinctive function in that context. Also, it's the isoform exclusively expressed in endothelial tissues in adults (Nohe *et al.*, 2005). Moreover, actin dynamics seems to be more disrupted when Cav-1 α is depleted in comparison to the depletion of Cav-1 β . In terms of their interacting partners, Cav-1 β , and not Cav-1 α , was shown to interact with bone morphogenetic protein (BMP) receptors, thus explaining in part the differential roles of the two isoforms. Finally, the presence of a distinctive phosphorylation site at tyrosine 14 in Cav-1 α , which upon mutation did not cause Cav-1 α to mimic Cav-1 β activity, contributes to the differential bio-functional roles of the two isoforms in signal transduction in cells. Interestingly, studies show that this site is phosphorylated in Cav-1 α in response to oxidative stress and that this modification is required for its proper functioning (Sun *et al.*, 2009).

3. Caveolin -1 in Mechanotransduction

Of particular relevance to this study is the identification of *CAV-1* as a mechanosensitive gene. Several studies have demonstrated its implication in mechanotransduction responses; most of which were reported in the context of endothelial cells and vascular smooth muscle cells. A number of studies have shown that different types of cells respond to mechanical stimuli, be it sheer stress or stretch, in a caveolin-dependent fashion. It has been reported that acute mechanical stress induced by osmotic swelling or by uni-axial stretching leads to a rapid disassembly of caveolae at the plasma membrane and a resultant increase in free caveolin. This response, which is an ATP - independent response, aims at releasing the tension that builds up as a result of mechanical stress. In muscular dystrophies, myotubes are more susceptible to mechanical stress and are more fragile due to the fact that they lack a functional built up of caveolae (Sinha *et al.*, 2011). In another study conducted in rat ventricular myocytes, caveolae restricted the activation of mechanosensitive channels in response to mechanical stretch/swelling by limiting the increase in tension in the membrane (Kozera *et al.*, 2009). Cav-1 also mediates the response of chondrocytes to mechanical overloading that produces hydrostatic stress, tensile strain, and fluid flow which ultimately leads to osteoarthritis (OA), a musculoskeletal disorder that is characterized by degeneration of cartilage. It has also been reported that Cav-1 and its binding partner toll like receptor (TLR4) respond to fluid sheer stress ultimately regulating NFkB interleukin 6 synthesis (Wang *et al.*, 2011). In vascular smooth muscles, the role of caveolin-1 has been extensively studied and has been demonstrated to regulate contractility, phenotype, and functional plasticity of vascular smooth muscles (Je *et al.*, 2004; Halayko *et al.*, 2008). In rat cardiomyocytes, stretch-induced activation of RhoA

and Rac1 depends on their localization in caveolae. Disrupting the latter leads to impairment of stretch-induced cytoskeleton reorganization and ERK translocation to the nucleus and it inhibits stretch-induced hypertrophy (Kawamura *et al.*, 2003). In fetal type II epithelial cells, Cav-1 translocates to the cytoplasm in response to stretch, and functions as a negative regulator of fetal type II epithelial cell differentiation where it decreases the stress-induced ERK phosphorylation and the mRNA levels of surfactant protein (SP-C), a specific marker for lung development (Wang *et al.*, 2010). In endothelial cells, Cav-1 senses the abrupt reduction of shear flow and stimulates the ROS mediated signaling pathway and endothelial cell proliferation (Milovanova *et al.*, 2008). In vascular wall, Cav-1 plays differential roles depending on the type of stress applied. For instance, the effects observed in response to pressure (stretch) do not rely on caveolin-1 by contrast to those observed in response shear flow whereby caveolin-1 has been reported to be implicated in Akt-dependent signaling in that it maintains basal ERK1/2 and Akt activity (Albinsson *et al.*, 2008).

4. Caveolin Knockout and Mutant Mouse Models

Caveolinopathies refer to a group of muscle diseases. One of well characterized gene causing these diseases is *CAV-3* that encodes for caveolin-3 which serves as a major component in caveolae in muscle cells. The phenotypes resulting from mutations in *CAV-3* are grouped into five categories, these are: 1) Distal myopathy, 2) hypertrophic cardiomyopathy, 3) Limb-girdle muscular dystrophy 1C (LGMD 1C), 4) Isolated hyperkalemia, 5) Rippling muscle disease (Pagon *et al.*, 2007). For in depth studies of the above diseases, a number of transgenic caveolin-3 mouse models have been generated, among which is the mutant P104L mutant caveolin-3 transgenic mouse

that serves as a model for autosomal dominant LGMD 1C (Ohsawa *et al.*, 2004). The study of such a model provided insight into the hearts of such mice that showed enhanced basal contractility and activation of endothelial nitric oxide synthase (e NOS) catalytic activity. Cav-1 has also been studied in that context. In fact, both Caveolin-1 and Caveolin-3 knockout mice also show an over activation in the MAPK pathway and suffer from cardiomyopathy (Cohen *et al.*, 2003; Woodman *et al.*, 2002). The hearts of the above mice models showed marked dilation of the right ventricular cavity and disrupted systolic function. Histological analysis confirmed hypertrophy of the cardiac myocyte along with interstitial fibrosis. It is worth mentioning, however; that caveolin - 1 study was not restricted to muscle disorders. In fact a number of studies investigated its role in other diseases among which is breast cancer. Several mutations in that context have been identified one of which is the caveolin-1 (P132L) which is expressed in 16% of breast cancer cases. This mutation ultimately prevents the proper targeting and localization of Caveolin-1, whereby misfolded caveolin-1 oligomers are retained in the Golgi complex (Lee *et al* 2002). Caveolin-2 knockout mice models on the other hand, show that Cav-2 acts as a negative regulator of proliferation of lung endothelial cells and the corresponding cell cycle progression. On the molecular levels, lung endothelial cells from caveolin-2 knockout mice show increased expression of cyclin A and cyclin B1 in addition to elevated expression of the inactive retinoblastoma protein, the G1 to S phase transition inhibitor (Xie *et al.*, 2010).

D. Hic-5

1. Overview of Hic-5

Hic-5 or Hydrogen peroxide-inducible clone 5 protein was first identified as a hydrogen peroxide inducible cDNA in mouse osteoblasts (Shibanuma *et al.*, 1994). It is also known as transforming growth factor beta 1 induced transcript, androgen receptor co-activator and as androgen receptor associated protein. Hic-5 functions in the nucleus and the cytoplasm and shuttles between both locations via an oxidant sensitive nuclear localization signal (NLS). At the level of the focal adhesion, Hic-5 functions as a molecular adapter that coordinates several protein – protein interactions, and has been implicated in the Wnt and TGF β signaling pathways where it acts as a positive regulator in the latter (Figure 4). Hic-5 also functions by targeting certain molecules, such as dopamine transporter SCLA3, to the plasma membrane and regulating their activity. By virtue of structural similarity and domain homology, Hic-5 is a member of the paxillin family. Like paxillin, Hic-5 is a member of group III subfamily of LIM domain proteins; both harboring four adjacent LIM domains in their C-terminus end and have shared LD motifs in the N-terminus end. They also share common binding partners including focal adhesion kinase (FAK), vinculin, and integrins and as such, they exhibit overlapping and antagonistic functions. Together they localize to the nucleus and to focal adhesions and link integrin mediated signaling to the nucleus (Caltagarone *et al.*, 2012). In the nucleus, Hic-5 regulates the activity of several transcription factors by functioning as a co-activator for the glucocorticoid, androgen, and progesterone receptor; thereby, regulating the expression of their downstream targets. In human fibroblasts, Hic-5 expression is induced during senescence and was shown to inhibit the growth of immortalized human fibroblasts. Moreover, the cellular proliferative capacity

of mouse embryonic fibroblasts (MEFs) was shown to be affected by Hic-5 expression levels as well as by its interaction with other cytoskeletal elements (Ishino *et al.*, 2000). In addition, Hic-5 acts as a negative regulator of fat cell differentiation. In C2C12 myoblasts, it was reported that Hic-5 plays a role in the initial stages of differentiation, whereby low levels of Hic-5 expression reduce the efficiency of myotube formation (Shibanuma *et al.*, 2002). Other studies however showed that Hic-5 along with DALP (Death Associated LIM-Only Protein), a Hic-5 orthologue in drosophila, act upstream of MyoD to block muscle differentiation and induce death (Hu *et al.*, 1999). The discordance in such conflicting reports could be attributed in part to the existence and the differential function of multiple Hic-5 isoforms. Twelve distinct isoforms of Hic-5 resulting from alternative splicing or alternative transcriptional start sites (TSS) were discovered in mouse tissues. These isoforms fall either into Hic-5 alpha (Hic-5 α) or Hic-5 beta (Hic-5 β) subfamilies; these differ at their N termini (LD motifs) while retaining an identical LIM domain. Thus, it is postulated that all isoforms might retain their ability to be targeted to focal adhesions and function as co-activators for nuclear receptors, while exhibiting differential binding to other interacting partners. The expression of these isoforms is spatially and temporally expressed, suggesting the distinct roles attributed to Hic-5. In myogenesis for instance, Hic-5 α was shown to permit myoblast fusion whereas Hic-5 β inhibits it (Gao *et al.*, 2005; Gao *et al.*, 2007). An additional factor that may contribute to the differential roles of Hic-5 isoforms is the presence of different putative phosphorylation sites. One of these differentially expressed sites for instance, regulates the interaction of Hic-5 with the androgen receptor. Finally, it is worth mentioning that the dimerization (hetero/homo) ability of Hic-5 isoforms and the resulting different dimers that could be formed adds up to the

complexity of their interaction and the resulting downstream signaling networks. Recently, it was shown that Hic-5 expression is regulated by the serum response factor (SRF) and myocardin-related transcription factor A (MRTFA), (Xiaobo *et al.*, 2011). Together SRF/MRTFA are key players in regulation of the differentiation, migration, and proliferation of muscle cells and their role in this respect has been widely investigated in smooth muscle cells.

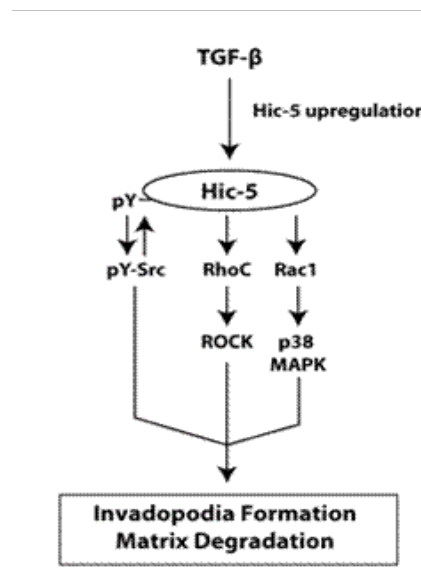


Figure 4: a schematic illustration of Hic-5 signaling in response to TGF- β stimulation that contributes to invadopodia formation and matrix degradation (Pignatelli *et al.*, 2012).

2. Hic-5 in Mechanotransduction

Of particular relevance to this study is the identification of *Hic-5* as a mechanosensitive gene and its implication in mechanically stimulated vascular wall remodeling. It has been reported that Hic-5 is a mediator of tensional force, where it regulates the contractile ability of cellular stress fibers by relocating from focal

adhesions to actin stress fibers upon stress loading in smooth muscle cells (Kim-Kaneyama *et al.*, 2005). Another example illustrating the role of Hic-5 as a mediator of mechanotransduction has been provided in vascular smooth muscles from Hic-5 deficient mice where upon wire injury of the femoral artery, the recovery of the arterial media was delayed due to apoptosis of vascular wall cells (Kim-Kaneyama *et al.*, 2011). Additionally, Hic-5 shuttling out of focal contacts in response to cyclic strain has been reported in osteoblast-like cells (Guignandon *et al.*, 2006). In small arteries, Hic-5 activation and association with Hsp27 was found to be involved in force development through inducing reorganization of actin cytoskeleton (Srinivasan *et al.*, 2008).

3. Hic-5 Ectopic expression and Knockout Mouse Models

To better understand the role of Hic-5, several studies attempted to either over express or silence Hic-5 and observe the resultant phenotype. The ectopic expression of Hic-5 in immortalized human fibroblasts induces senescence –like phenotype in comparison to delayed senescence in cells expressing antisense *Hic-5* RNA (Shibanuma *et al.*, 1997). In mouse embryonic fibroblasts, the over expression of Hic-5 reduced cell spreading via competing for FAK with paxillin. The phenotype can be reversed by expressing anti sense *Hic-5* RNA in these MEFs (Nishiya *et al.*, 2001). In rat calvarial cells RCT-1, forced expression of Hic-5 leads to decreased proliferation and enhances the differentiation- related phenotype (Shibanuma *et al.*, 1998). In addition to ectopically modulating the expression of Hic-5, mice models deficient for Hic-5 have also been generated. Although *Hic-5* null mice are viable and fertile, smooth muscle cells derived from these mice are more susceptible to stretch induced apoptosis. Moreover, following wire injury, the recovery of the femoral artery was delayed,

suggesting that the induced apoptosis observed in the vascular smooth muscle cells due to absence of Hic-5 may result in that (Kim-Kaneyama *et al.*, 2011).

E. Laminopathies and Oxidative Stress

Reactive oxygen species (ROS) are small molecules that are produced by the cell and persist for a short time. These molecules mediate a number of biological processes ranging from gene expression, differentiation, migration and proliferation. In some cases; however, ROS accumulation can lead to oxidative stress. This happens when ROS production is increased and/or when the antioxidant defense is hindered (Sieprath *et al.*, 2012). Enzymes that catalyze the processing of ROS products including catalase (CAT), superoxide dismutase (SOD), and glutathione peroxidase (GPX) comprise the antioxidant system that the eukaryotic cell has developed to prevent damage. The redox state of the cell affects a number of processes; on top of which is gene expression. At the level of cellular processes, five main categories are affected; these are: 1) modulation of cytokine, growth factor, or hormone action and secretion, 2) ion transport, 3) transcription, 4) neuromodulation, and 5) apoptosis (Lander *et al.*, 1997). The Mitogen-Activated Protein Kinase (MAPK) and NF- κ B pathways are the most studied redox sensitive pathways. The activation of MAPK pathway ultimately regulates the activity of numerous transcription factors thereby bridging extracellular signaling and cell surface receptor on one hand and targeted gene expression on the other (Su *et al.*, 1996). Acute phase proteins, cell surface receptors, and cytokines all are regulated by NF- κ B signaling (Ginn-Pease *et al.*, 1998).

Altered levels of ROS accompanied with an amped cellular susceptibility to oxidative stress have been reported in laminopathies (Sieprath *et al.*, 2012). Cells derived from laminopathy patients exhibited increased levels of ROS, and were more prone to oxidative stress. Moreover, the levels of antioxidant enzymes were influenced by the varying levels of mature lamin A and the function of mature lamin A was affected by its oxidation state. It was shown that an oxidized mature lamin A has perturbed activity which contributes to senescence in cells vulnerable to ROS species (Pekovic *et al.*, 2011). Accordingly, in the context of laminopathies, ROS act by inducing senescence. Telomere shortening is prevalent under oxidative stress conditions; it was also found to be the case in fibroblasts harboring *LMNA* mutations (Richter *et al.*, 2007). Hence, in laminopathies, elevated levels of oxidative stress induce telomere shortening which in turn promotes cellular senescence through activation of p53 (Sieprath *et al.*, 2012).

To understand the perturbed redox biology in the context of laminopathies and dysfunctional lamina, it is imperative to point out to the numerous key roles that are played by the nuclear lamina and the detrimental effects which result from an aberrant nuclear lamina. As mentioned earlier, the nuclear lamina controls gene expression through interaction with chromatin and with a wide panel of transcription factors. Some of these transcription factors such as Rb, SREBP1, and Oct1, are redox responsive; therefore, a dysfunctional lamina affects the redox response of cells. Moreover, an intact nuclear lamina is also implicated in forming an intact nuclear envelope which serves to ensure proper compartmentalization of the cell. An impaired nuclear lamina may lead to delocalization of certain cytoplasmic components into the nucleus, some of which might

be sources of ROS species including the mitochondria. As a consequence, the DNA is more susceptible to oxidative damage and the cell is more susceptible to senescence (De Vos *et al.*, 2011). It is also worth noting that the nuclear lamina is a part of a proposed “nuclear shield” that accumulates antioxidant enzymes and helps protect DNA from oxidative damage (Fabrini *et al.*, 2012), and in what seems to be a link between lamins, oxidative stress and mitochondria, both lamin A and lamin B1 were also reported to affect the function of the mitochondria by regulating the expression of key elements of the mitochondrial functions including certain enzyme complexes involved in ROS production.

F. Gap in Knowledge, Rationale, and Hypothesis

To date, the molecular mechanisms underlying the phenotypic diversity in laminopathies have not been deciphered; in particular how mutations in a single ubiquitously expressed gene lead to tissue specific phenotypes. Many hypotheses have been proposed of which two stand out the most. These are the “**structural hypothesis**” and the “**gene-regulation hypothesis**” (Figure 5). We are interested in the gene regulation theory that proposes that altered tissue-specific gene expression and regulation may underlie the development of different disease phenotypes. Our focus will be on the gene-regulation theory in relation to mechanosensitive genes; i.e. genes that respond to mechanical stress and translate mechanical forces into biochemical signals (Nowlan *et al.*, 2008; Jaalouk *et al.*, 2009). This interest stems out from the fact that muscular laminopathies, as is the case for many laminopathies, are primarily manifested in mechanically stressed tissues.

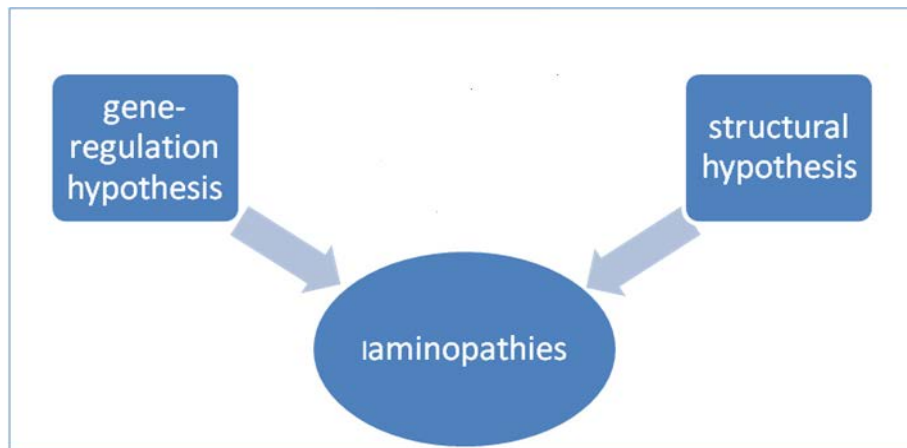


Figure 5: Two main theories have been proposed to explain the underlying phenotypic diversity in laminopathies namely the “gene-regulation hypothesis” and the “structural hypothesis”.

Our choice to study the *CAV-1* and *Hic-5* genes was based on three main criteria. In the context of muscular laminopathies, we are interested in investigating mechanosensitive genes that: 1) have been reported to be involved in mechanotransduction and that are also affected by oxidative stress, 2) have been shown to play a key role in muscle cell biology and in myogenesis and for which KO/mutant models show a phenotype similar to that of *LMNA* KO/mutant models, and 3) have not been studied yet in muscular laminopathies. Taking these three criteria together, we narrowed down the panel of putative mechanosensitive genes from which we decided to focus on *CAV-1* and *Hic-5*. To date, the role of caveolin gene family (including *CAV-1*) and that of *Hic-5* in muscular laminopathies have not been studied. In view of their signaling cross-talk (Razani *et al.*, 2001) and their reported role in mechanotransduction in cellular response to changes in the stiffness of the extracellular matrix or alterations in cell-generated tension (both responses shown to be altered in muscular laminopathies), we hereby hypothesize that there is dual deregulation of *CAV-1* and

Hic-5, in terms of modulated expression levels and/or alterations in intracellular distribution, in muscular laminopathies.

G. Objective of the Study and Specific Aims

Our long-term objective is to test if the expression levels of *Cav-1* and *Hic-5* are deregulated in muscular laminopathies and whether such deregulation may be contributing to the pathogenesis of the disease. For the purpose of this study (short-to-midterm), our **specific aims** are:

Aim 1: to determine whether *Cav-1* and *Hic-5* are differentially expressed at the transcriptional level in mouse embryo fibroblasts (MEFs) derived from mouse models of muscular laminopathies in comparison to wild-type controls cultured *in vitro* under baseline conditions.

Given the technical hurdles associated with and the high cost of culturing and maintaining myocytes, we will be using immortalized MEFs derived from a mouse model of EDMD that is Lamin A/C - deficient (*Lmna*^{-/-}) and MEFs derived from a knock out/knock in mouse model of DCM that expresses *Lmna*^{N195K/N195K}. MEFs derived from wild-type littermates (*Lmna*^{+/+}) will be used as controls. These cell lines are a generous gift provided by Dr. Jan Lammerding (Cornell, NY). The two mechanosensitive genes we are interested in are: *i) Cav-1* gene that encodes for caveolin-1 α and caveolin-1 β , and *ii) Hic-5/TGFB1/1* gene that encodes for transforming growth factor beta 1 induced transcript. Additionally, expression levels will be quantified for the house keeping gene *18s* encoding for 18s ribosomal subunit. The transcriptional levels of the selected mechanosensitive genes normalized to the house

keeping gene(s) will be quantified in the panel of MEFs cultured *in vitro* under baseline conditions.

Aim 2: to assess whether Cav-1 and Hic-5 are differentially expressed at the protein level in MEFs derived from mouse models of muscular laminopathies in comparison to wild-type controls cultured *in vitro* under baseline conditions.

We will use immunofluorescence staining and microscopic imaging of PFA-fixed, and Triton permeabilized cells to examine differences in the expression of Cav-1 and Hic-5 at the protein level in the MEFs cell line panel. Additionally, we intend to look for any alterations in the intra-cellular distribution of these proteins that may be exhibited between the different cell lines. Briefly, PFA-fixed cells will be blocked then stained with select primary antibody recognizing a protein of interest, followed by secondary antibody detection. Cells stained with secondary only will be used as controls. To assess any modulation in mechanosensitive gene expression levels of the corresponding proteins, we will also use standard Western Blot analysis of protein extracts from samples of MEFs cell lines cultured *in vitro* under baseline conditions. Expression levels will be quantified by densitometry and normalized to GAPDH loading controls.

Aim 3: to investigate the effect of oxidative stress on the expression profile of *CAV-1* and *Hic-5* in MEFs derived from mouse models of EDMD and DCM in comparison to wild-type controls.

Cells will be subjected to stress induced by hydrogen peroxide (H₂O₂) of 0.1 and 0.5 μ molar concentrations for variable time points ranging from 5 minutes to 1hour.

Subsequent to stress application, sample RNA extractions will be performed followed by Real-Time PCR for quantification of stress-induced gene expression of the select mechanosensitive genes mentioned above. RNA extracted from untreated cells will be used as controls.

CHAPTER II

MATERIALS AND METHODS

A. Cell Culture

1. *Lmna* WT MEFs (*Lmna*^{+/+})

Lmna^{+/+} MEFs are immortalized mouse embryonic fibroblast cells derived from wild-type littermates (Stewart C *et al* 1993). The cell line was kindly provided by Dr. Jan Lammerding (Cornell, NY). It has been very well characterized in terms of Lamin A/C expression (Zwerger *et al.*, 2013; Lammerding *et al.*, 2004; Lombardi *et al.*, 2011). *Lmna*^{+/+} MEFs were cultured using Dulbecco's Modified Eagle's Medium DMEM-AQ media (Sigma), supplemented with 1% penicillin- streptomycin and 10% Fetal bovine serum(FBS). *Lmna*^{+/+} MEFs double in about 24 hours; when 80% confluent density is reached, cells were washed with 1× Dulbecco's Phosphate Buffered Saline (DPBS) (GIBCO-Invitrogen) then with 1×Trypsin (Lonza) to detach them from the plate, incubated for 5 min in an incubator at 37°C and 5% CO₂. Then, cells were washed with re-suspension media to neutralize the effect of trypsin, centrifuged for 5 min at 4°C at 600 g. Afterwards, the pellet was re-suspended with the needed amount of media to be distributed in tissue culture plates that were pre-filled with media. Cell counting was done using trypan blue vital exclusion stain.

2. *Lmna* Null MEFs (*Lmna*^{-/-})

Lmna^{-/-} MEFs are immortalized mouse embryonic fibroblasts derived from a mouse model of EDMD that is Lamin A/C-deficient (Sullivan *et al* 1999). The cell line

was kindly provided by Dr. Jan Lammerding (Cornell, NY). It has been very well characterized in terms of Lamin A/C expression (Zwerger *et al.*, 2013; Lammerding *et al.*, 2004; Lombardi *et al.*, 2011). The cells were propagated in tissue culture similarly as the *Lmna*^{+/+} MEFs. These cells exhibit distinct nuclear morphology in that they have irregularly shaped nuclei. They also double faster than their corresponding wild type controls.

3. *Lmna*^{N195K/N195K} MEFs

Lmna^{N195K/N195K} MEFs are immortalized mouse embryonic fibroblasts derived from a knock out/knock in mouse model of DCM that expresses the N195K mutant form of A-type lamins (Mounkes *et al* 2005). The cell line was kindly provided by Dr. Jan Lammerding (Cornell, NY). It has been very well characterized in terms of Lamin A/C expression (Zwerger *et al.*, 2013; Lammerding *et al.*, 2004; Lombardi *et al.*, 2011). The cells were propagated in tissue culture in a similar fashion to the above mentioned cell lines. As it is the case with *Lmna*^{-/-} MEFs, these cells have a shorter doubling time (i.e. proliferate faster than WT cells) and their nuclei are elongated in compared to the oval shaped nuclei of WT MEFs.

B. RNA Extraction

RNA samples were extracted from *Lmna*^{+/+}, *Lmna*^{-/-}, and *Lmna*^{N195K/N195K} MEFs under the following conditions:

1. Baseline Conditions

Cells were seeded in 6-well plates at a density of 2×10^5 cells per well in serum supplemented media. When they reached ~80% confluence, they were washed with 1xPBS and RNA was extracted using RNeasy Kit (QIAGEN) according to manufacturers' specifications. All RNA samples were stored at -80°C . The quantity and the quality of the extracted RNA samples were assessed using Nanodrop Spectrophotometer (Thermonanodrop 2000C). RNA extracted from *Lmna*^{+/+} MEFs samples would serve as reference for gene expression.

2. H₂O₂- Induced Stress

Cells were seeded in 6-well plates at a density of 2×10^5 cells per well in serum supplemented media. When they reached ~80% confluence, cells are treated with either 0.1 μM H₂O₂ (hydrogen peroxide solution-36.5-34.5 %- Sigma-Aldrich) or 0.5 μM H₂O₂ for 5, 15, 30 minutes or 1 hour. After treatment, cells were rinsed once with 1x PBS and RNA extraction was performed using RNeasy Kit (QIAGEN) as mentioned above. Untreated cells (within each cell line) corresponding to each time point were used as reference.

C. Reverse Transcription

1 μg of RNA from each sample was used to reverse transcribe into cDNA using iScript cDNA Synthesis Kit (Bio-Rad). Accordingly, 1 μg of the RNA samples was mixed with 1 μl of the reverse transcriptase enzyme in addition to 4 μl of the Reaction Mix and adjusted to a total volume of 20 μl with Nuclease free sterile water

(AMRESCO). The reaction to cDNA was initiated in the DNA engine machine (Peltier thermal cycler, Bio-Rad). The protocol consists of 5 min at 25°C, followed by 30 min at 42°C eventually for 5 min at 85°C (state which one is the annealing temp....etc). All cDNA samples were stored at -20°C.

D. Real -Time PCR

iQ SYBR Green Supermix (Bio-Rad) was used to perform the Real-Time PCR amplification using specific primer pairs for each gene. The following previously validated primer sequences for the Real-Time PCR amplification of select mechanosensitive genes were computationally derived from the MGH/Harvard Medical school primer Bank Database, using the following site

(www.pga.mgh.harvard.edu/primerbank). Table 2 lists the primer sequences that were used for Real-Time PCR quantification of each gene.

Table 2: A list showing the sequences of the forward and the reverse primers that were used to quantify the transcriptional expression of the α isoform of *CAV-1*, *Hic-5*, and the *18S* reference gene by Real-Time PCR.

| Gene | Primer Sequences |
|---|---|
| <i>CAV-1</i> (amplifies the α isoform only) | Forward Primer: 5'- GCGACCCTAAACACCTCAAC-3' Reverse Primer: 5'-ATGCCGTCAAACTGTGTGTC-3' |
| <i>HIC-5</i> | Forward Primer: 5'-TACAGCACGGTATGCAAGCC-3' Reverse Primer: 5'- GCAACCGATCTAGCTCACAGAG-3' |
| <i>18S</i> | Forward Primer:5'-TCAAGAACGAAAGTCGGAGG-3' Reverse Primer: 5'-GGACAT CTAAGG GCATCACA-3' |

The reverse transcribed cDNA was diluted 1:20 by adding 5 μ l cDNA to 95 μ l nuclease-free sterile water. For each 4 μ l diluted cDNA derived from the different samples, we added 1 μ l forward primer and 1 μ l reverse primer (for each gene), in addition to 6.5 μ l nuclease-free sterile water and 12.5 μ l Mastermix to a total volume of 25 μ l. The reaction was carried on using a Real-Time PCR machine(c-1000 Touch thermal cycler, Bio-Rad). The protocol used consists of the following steps: an initial heating step to 50°C followed by an increase to 95°C for 10min for DNA denaturation step, the primers anneal to their complementary strand by lowering the temperature to 60°C for 1min, the extension step was performed at a temperature of 72°C for 30 seconds; this process was repeated for 40 cycles. The final extension step was for 10 min at 72°C. Experimental results were recorded and analyzed using the Bio-Rad CFX Manager Software.

E. SDS-PAGE & Western Blot Analysis

1. Protein Extraction

Cells were seeded in complete media in 10cc dishes. When they reached 80% confluence, they were washed with 2x pre-cooled PBS (-) or HBSS (-) using ~3-5ml/10cc dish (depending on cell density). 0.3-0.5ml RIPA lysis buffer (Sigma-Aldrich) was added per sample (depending on cell density); the buffer was supplemented with Protease Inhibitors (Sigma P-8340 protease inhibitor cocktail). Samples were incubated in the cold room shaker for 30min. Cell scraper and/or micropipette tip was used to lodge off any lysate clusters. The cell lysates were then transferred to pre-cooled sterile microfuge tubes and were centrifuged at 13600 rpm at 4°C for 10min. Each of the supernatants (containing the protein extracts) was then transferred to a labeled, pre-cooled microfuge tube. Samples were finally stored at -20 or -80°C (depending on the nature of the protein(s) we aimed to quantify by Western Blot analysis).

2. Sample Protein Quantification

We used 96-well plates; the first two lanes were used for standardization using specific dilutions of 1mg/ml of bovine serum albumin (BSA) in dH₂O. Standards were made (in duplicates) with the following protein content (in µg): 0.0, 0.5, 1.0, 2.0, 4.0, 6.0, 8.0, and 10.0. Then, 5µl of each sample were placed in subsequent rows (in duplicates). Finally, 200µl of Optiblot Bradford Reagent (Abcam, ab119216) were added to each well and measurement of protein contents was performed using the SpectraMax ascent software (Multiskan EX, Thermo lab Systems).

3. SDS-PAGE; Preparing & Running the Gel

For 25-75KDa proteins, we used 4-12% Bis-Tris with 1x running buffer. 10x running buffer was prepared by adding 25g of Tris -base (Bio-Rad), 144g of glycine (Bio-Rad), 10g of full name (SDS) (Bio-Rad), then H₂O for a final volume of 1L. Then the latter solution was diluted by a dilution factor of 1:10 to get a final concentration of 1x running buffer. As for the 10-well gel, it was prepared with 0.75mm thickness. The casting and running apparatus were kindly provided by Dr. Rabih Talhouk's laboratory. The lower (running) gel was prepared by adding 1600 µl acrylamide (Bio-Rad), 1000µl of resolving buffer Tris-HCl (Bio-Rad), and 1400µl of double distilled H₂O. It was then mixed with 70 µl of APS and 10 µl of TEMED (Bio-Rad) for 45 min to allow the gel to solidify. Then, we prepared the upper or stacking part of the gel by adding 375 µl of acrylamide, 625 µl stacking buffer, and 1525 µl of double distilled H₂O. It was then mixed with 70 µl of APS and 10 µl of TEMED for 15 min to solidify after having placed the combs half way through adding the mixture. While the gel as solidifying, we then added the appropriate amount of 5x loading buffer with betamercaptoethanol (BME) to 10µg of protein sample so that final sample volume was ~ 20-25 µl. The samples were then denatured by boiling at 95°C for 5min using a heat block, placed directly on ice to prevent re-folding. The samples were briefly spun to remove water condensation. We then loaded the gel with 10ul of protein standard (Fermentis-Page Ruler-pre-stained protein ladder), in addition to the protein samples. The gel was placed in a gel box with the loading side facing inwards, with the holder placed on the opposite side, the gel box was locked.

1x running buffer was used while ensuring that the gel seals tightly and that the outer chamber was partly or fully filled. The comb was carefully removed and the gel

was run at 200V for ~1h or until the leading edge/loading dye reached bottom of the gel. Meantime, we placed the gel-running box in an ice bucket after a few minutes to avoid over heating.

4. Protein Transfer from Gel to Blot

Transfer membrane blot (NEN LifeScience, PolyScreen PVDF TransferMembrane) was cut to the desired size of the gel. We used blotting paper as reference for size. Carefully, the protective sheet was removed without touching the membrane; placed membrane in 5ml of 100% methanol to activate for ~1min (this step was done under the fume hood). The gel was removed from the reservoir a metal spatula was used to release the gel from the holding covers. The gel was carefully soaked in pre-cooled 1x transfer buffer in a small container. The transfer buffer was prepared by adding 2.5g of Tris-base to 14.4g of glycine, supplemented with 200ml of methanol, then added dH₂O for a final volume of 1L. Extra-thick blot papers (Bio-Rad) and the cut-out membrane blot were also soaked in 1x transfer buffer. In a Trans-Blot SD Semi-Dry Transfer Cell (Bio-Rad), extra-thick blot papers were placed, and then methanol-activated membrane was placed on top, followed by the gel, and then the 2nd extra-thick blot paper. Some transfer buffer was poured to saturate the paper and to ensure there that there were no bubbles. The apparatus lid was tightly closed and the setup was run at 25V for ~30min. Afterwards, the thick blotting papers and the gel were properly discarded in polyacrylamide waste container and the membrane blot was soaked in 10ml wash buffer of 0.1% PBS-T to wash on a shaker for a few minutes before the blocking step. The wash buffer was prepared by using regular PBS (non-sterile) without Ca, Mg, adjusted to pH7.2 and adding Tween-20 (Polyoxyethylene Sorbitan Monolaureate, Sigma-Aldrich), at a final concentration of 0.1%, i.e. 1ml of Tween for 1L of PBS.

5. Western Blot Analysis; Blocking, Washing Steps, & Antibody Incubations

The membrane was transferred into a blotting case with ~10ml of 5% milk prepared in 0.1% PBS-T. It was then incubated on a shaker (slow) for ~1-2h at RT for blocking. The blocking solution was prepared by measuring 5g of non-fat milk powder (supplier) and adding it to 100ml of 0.1% PBS-T and stirring for few minutes.

The primary antibodies that were used in this study are: Caveolin-1 antibody (N-20-sc-894; rabbit IgG, 200µg/ml, used at 1:500, Santa Cruz Inc.); Hic-5 antibody (H-75-sc-28748; rabbit IgG, 200µg/ml, used at 1:500, Santa Cruz Inc.); and GAPDH antibody (FL-335- sc-25778; rabbit IgG 200µg/ml, used at 1:500, Santa Cruz Inc.). Following blocking, the membranes were placed in cases and incubated with primary antibody diluted in ~5ml of 5% milk/0.1% PBS-T at 4°C on shaker (slow) overnight. The next day, the membranes were washed 3x using 10ml of 0.1% PBS-T on the shaker (fast) at RT for 10min, then secondary antibody incubation was done using alpha 488 (goat anti rabbit IgG; 0.8µg/µl; Jackson Immunoresearch) diluted in ~5ml of 5% milk in 0.1% PBS-T at 1:2500; then incubated on shaker (slow) at RT for 1-2hrs. Finally, the membranes were washed 3-4x using 10ml of 0.1% PBS-T on shaker (fast) at RT for 10min.

6. Western Blot Analysis; Developing Step

A working solution of Western Lightening Chemiluminescence Reagent (ECL Western Blot Substrate, Abcam) was prepared by mixing 1ml of Reagent A with 1ml of Reagent B. Then, the probed membranes were placed in cassette (Spectroline-monotec

cassette, Spectronics Corporation) with Western Lightning Chemiluminescence Reagent (Abcam) for 1 min; a plastic pouch was taped into the cassette and the membrane was placed in pouch with a specific noted orientation. An autoradiography X-ray film (AGFA or Fujifilm) was inserted into the cassette in the dark room and the film was exposed for 30 sec, 1 min, 5 min, etc., and developed using XOMAT X-ray film processor (Optimax).

7. Membrane Stripping for Probing with a Different Antibody

If need be, the antibody probed membranes were stripped using 10ml of 0.1N NaOH, for 45 min at RT. This step removes antibodies and some protein. Then, the membranes were washed 1-2x with 10ml of 0.1% PBS-T or 0.1% TBS-T for a few minutes. Incubation with a second antibody of interest such as GAPDH antibody was then performed following the same procedure used previously with minor modifications; first blocked in ~5ml of 5% milk/0.1% PBS-T at RT for 1-2 hours, then incubated with primary GAPDH antibody (FL-335-sc-25778; rabbit IgG, 200ug/ml, 1:500, Santa Cruz Inc.) at RT for 1 hour. Then, membranes were washed 3x using 10ml of 0.1% PBS-T on shaker (fast) at RT for 10min followed by secondary antibody incubation and wash steps as previously stated.

F. Immunofluorescence Staining

Each cell line was seeded in a 12-well plate at 1:5 in 0.5ml per well of complete DMEM-AQ media supplemented with FBS and Pen/Strep. The cells were left to adhere overnight or for 2 days at 37°C, 5% CO₂, i.e. until they reached 80% confluence. Then, cells were washed 2x with PBS, 5 min each, and fixed with 4%

Paraformaldehyde (PFA, Sigma-Aldrich) in PBS (500 μ l per well) at RT for 20 min. The 4%PFA solution was prepared by diluting stock of 16% PFA using PBS. We then washed 3x with PBS; a quick first wash followed by 2 washes 5 min each and permeabilized with 0.2% Triton in PBS (500 μ l per well) for 10 min. To prepare 0.2% of Triton (Sigma-Aldrich), we proceeded first by preparing a transitional dilution of 10% from the original stock of 100% by adding 10 μ l of 100% Triton in 900 μ l of PBS. The required volume of 0.2% of Triton (based on number of samples) was then prepared by diluting the above in PBS. We then washed as mentioned above and continued by blocking with 2% BSA in PBS (500 μ l per well) on nutator for 2 hrs; prepared 2%BSA in PBS by diluting the stock of 10% BSA in PBS . The blocking media was then removed followed by washing 1x with PBS. For incubation with primary antibody rabbit anti-caveolin-1 (N-20-sc-894,200 μ g/ml), the latter was diluted at 1:200 in 1%BSA in PBS and 500 μ l were added per well and placed on nutator for 2 hrs; prepared 1% BSA in PBS by diluting stock of 10% BSA in PBS. Then, we washed 3x with PBS for 5 min each on nutator and incubated with secondary antibody Alexa Fluor 594-conjugate (Affinity purified, goat anti rabbit IgG (H+L), 1.5 μ g/ μ l, Jackson ImmunoResearch) diluted at 1:200 in PBS only; 500 μ l were added per well and left for 1 hr on the nutator. This step was followed by 2 wash steps with PBS, 5 min each, on nutator. For nuclear staining, the samples were incubated with Hoechst (trihydrochloride trihydrate, Invitrogen, Molecular Probes) diluted at 1:3000 in PBS only; 500 μ l per well on nutator for 30 min. Finally, 2 wash steps with PBS were performed for 5min each on nutator and the samples were covered with syran wrap and foil and then stored 4°C for microscopic imaging.

G. Microscopic Imaging

Stained cells were left for 48 hours at 4°C after which they were observed and imaged using fluorescence microscope (Olympus microscope, Axiovert 200, Zeiss). Standard phase-contrast microscopic images were acquired to assess the overall confluence, integrity, and spreading of cells. Then fluorescent images were acquired with 40x magnification (exposure times were 141.64, 110.77, and 1500msec for FS42, FS02, and FS14 respectively). The corresponding excitation wavelengths were 450nm and 510nm.

H. Image J analysis

The fluorescence intensity for each cell in a particular image frame was quantified using Image J 1.41 free Java image processing program software. The software was downloaded from an online application source that is made available for the public (rsbweb.nih.gov).

I. Statistical Analysis

The statistical analysis was done using 2 - tailed student t-test. The calculations were performed using Microsoft Excel program. The statistical significance is represented by a p-value of 0.05 with a highly significant difference at 0.01. Calculations of the standard deviation (STDEV), and the standard error of the mean (SEM) were done following calculation of the average compared to a control.

CHAPTER III

RESULTS

Aim 1: to determine whether *Cav-1* and *Hic-5* are differentially expressed at the transcriptional level in mouse embryo fibroblasts (MEFs) derived from mouse models of muscular laminopathies in comparison to wild-type controls cultured *in vitro* under baseline conditions.

1.1 Our data show that Cav-1 alpha gene expression is down-regulated in Lmna^{-/-} MEFs (Lamin A/C null) and in Lmna^{N195K/N195K} MEFs in comparison to Lmna^{+/+} MEFs controls

We aimed to determine the transcriptional expression levels of *Cav-1* gene at baseline conditions in *Lmna^{-/-}* MEFs and in *Lmna^{N195K/N195K}* MEFs. Under baseline conditions and when normalized to the transcriptional levels of the *18S* reference gene, the expression of *Cav-1* α in Lamin A/C null MEFs was 0.48 –fold (± 0.18) of that of the control WT MEFs, reflecting more than 50% decrease in transcript expression that was borderline significant ($P = 0.05$). Likewise, *Cav-1* α transcript expression was significantly decreased in *Lmna^{N195K/N195K}* MEFs in that it was 0.51 –fold (± 0.16) in comparison to WT MEFs ($P = 0.04$). Results represent average \pm SEM of three independent experiments, each done in duplicates (Figure 6). Our preliminary results also suggest a similar down-regulation in the transcriptional levels of the β isoform of

Cav-1 in the Lamin A/C null and the N195K mutant MEF cell lines in comparison to WT controls (data not shown; pending further validation).

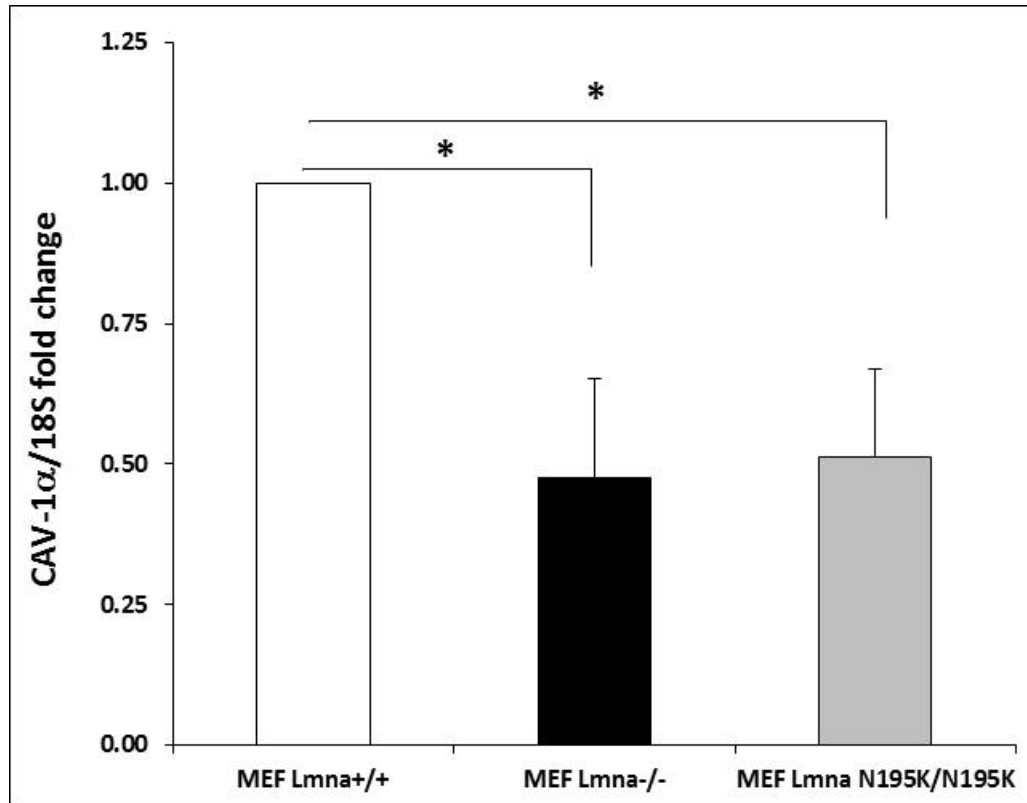


Figure 6: *Cav-1 α* gene expression in *Lmna*^{-/-} MEFs and *Lmna*^{N195K/N195K} MEFs cells at baseline conditions. Our data indicate that *Cav-1 α* transcript expression is down-regulated in MEFs deficient in A-type lamins and in MEFs expressing the N195K mutant form. *Cav-1 α* transcript expression was normalized to that of the *18S* reference gene. Data represent mean fold difference \pm SEM in comparison to WT controls; derived from 3 independent experiments, each performed in duplicates. One asterisk represents statistical significance ($p < 0.05$).

1.2 Our data suggest that Hic-5 gene expression is up-regulated in Lmna^{-/-} MEFs

(Lamin A/C null) and in Lmna^{N195K/N195K} MEFs in comparison to Lmna^{+/+} MEFs wild- type controls

We aimed to determine the transcriptional expression levels of *Hic-5* gene at baseline conditions in *Lmna^{-/-}* MEFs and in *Lmna^{N195K/N195K}* MEFs. Under baseline conditions and when normalized to the transcriptional levels of the *18S* reference gene, the expression of *Hic-5* in Lamin A/C null MEFs was 1.75 – fold (± 1.01) of that of the control WT MEFs, suggesting ~75% increase in transcript expression. However, despite the marked up-regulation, this increase was determined not to be statistically significant ($P > 0.05$) likely due to the large deviation we obtained in multiple independent experiments and the sensitivity of *Hic-5* expression to culture conditions including cell confluence and cell –cell contact. Likewise, a 1.94 -fold (± 0.70) increase in *Hic-5* expression was noted in *Lmna^{N195K/N195K}* MEFs in comparison to their WT counterparts. However, as was the case for Lamin A/C null MEFs, the marked up-regulation in *Hic-5* transcript expression that was noted in the N195K mutant MEFs was not statistically significantly different from the control. Results represent mean fold \pm SEM derived from three independent experiments, each done in duplicates (Figure 7).

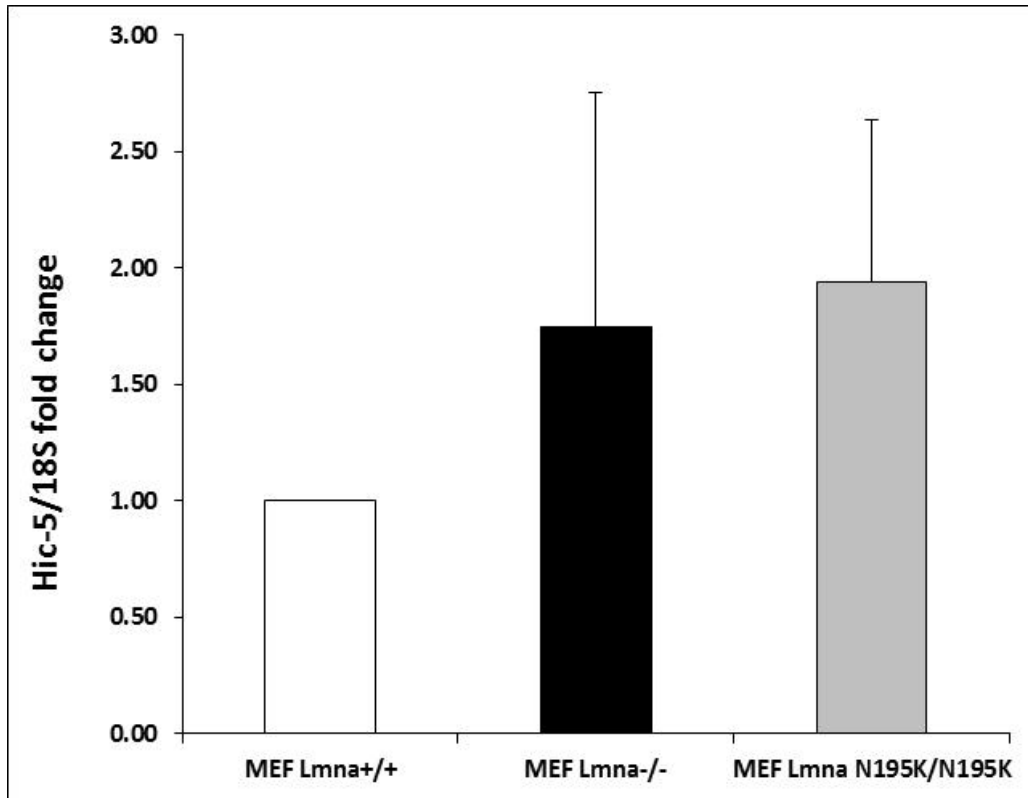


Figure 7: *Hic-5* gene expression in *Lmna*^{-/-} and in *Lmna*^{N195K/N195K} MEF cells quantified at base-line conditions and plotted post normalization to the transcript levels of the *18S* reference gene. Our data suggest a marked elevation in *Hic-5* gene expression in MEFs deficient in A-type lamins and in MEFs expressing the N195K mutant form. Data represent mean ± SEM derived from 3 independent experiments, each performed in duplicates.

Aim 2: to assess whether Cav-1 and *Hic-5* are differentially expressed at the protein level in MEFs derived from mouse models of muscular laminopathies in comparison to wild-type controls cultured *in vitro* under baseline conditions.

2.1 Immunofluorescence staining of caveolin-1a shows no significant difference in protein expression levels in *Lmna*^{-/-} and *Lmna*^{N195K/N195K} MEFs compared to *Lmna*^{+/+} wild-type controls

We aimed to assess the protein expression levels of the α isoform of caveolin-1

under baseline tissue culture conditions in MEFs deficient for A-type lamins and those expressing the N195K mutant form. Accordingly, we performed immunofluorescence staining of PFA fixed cells which were then stained using Cav-1 α antibody. Multiple image frames were then acquired using same exposure for all three cell lines. Subsequently, images were analyzed using Image J software whereby we did a relative semi-quantitative assessment of Cav-1 α per cell per frame by measuring the relative fluorescence intensity normalized to background between the various samples. Our results show that, under baseline conditions, there is no significant difference in protein expression of the alpha isoform of caveolin-1 between the two mutant cell lines and the WT control (Figure 8); a set of representative images are shown in Figure 10 (upper panel). Quantifying fluorescent staining of Cav-1 α , a 1.03-fold (± 0.10) insignificant difference in relative fluorescence intensity was obtained in Lamin A/C deficient MEFs in comparison to MEFs expressing WT Lamin A/C ($P > 0.05$). Likewise, a 1.14-fold (± 0.08) insignificant difference in relative fluorescence intensity was obtained in MEFs expressing the N195K mutant form in comparison to control WT cells ($P > 0.05$). Results represent mean fold change \pm SEM of three independent experiments. Using J software, \sim 50 cells per cell line were analyzed from different image frames per experiment amounting to an average total of 150 cells per cell line.

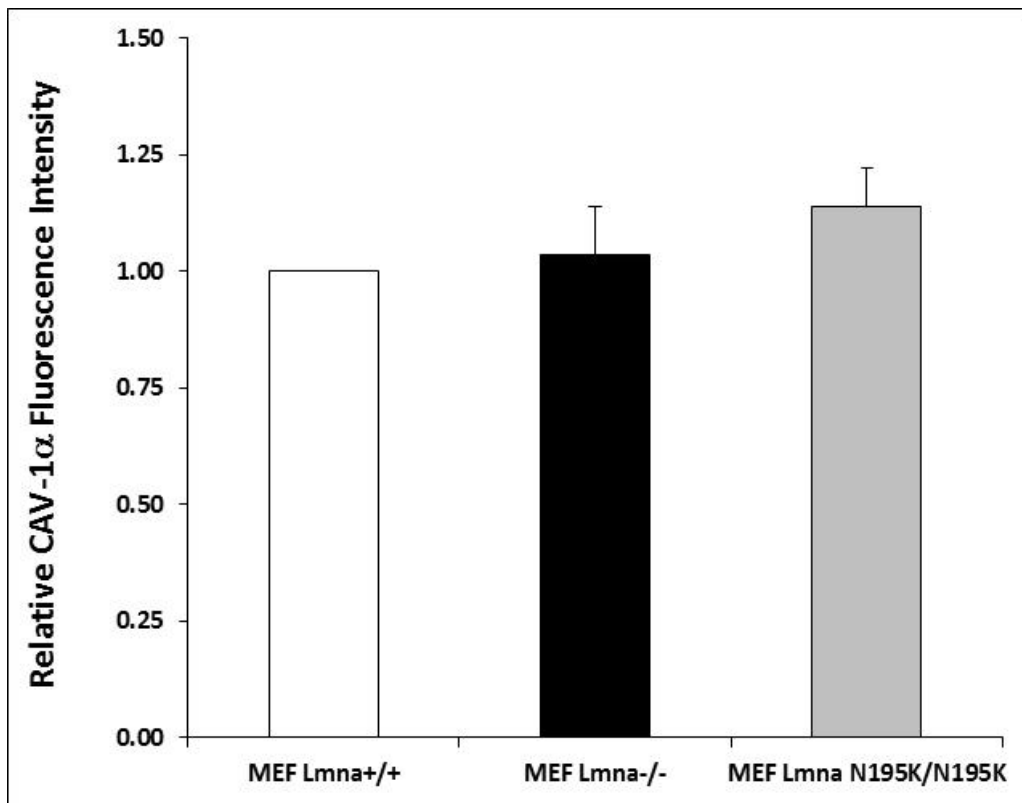


Figure 8: a semi-quantitative assessment of the relative fluorescence intensity of Cav-1 α immunostaining in *Lmna*^{-/-} and in *Lmna*^{N195K/N195K} MEF cells in comparison to WT control MEF cells at baseline conditions shows no significant difference in expression between the three cell lines. Data represent mean \pm SEM derived from 3 independent experiments. An average total of 150 cells per cell line were analyzed using image J software.

2.2 Immunofluorescence staining of Hic-5 protein indicates no significant difference

*in steady state protein expression levels in *Lmna*^{-/-} MEFs (Lamin A/C null) and in *Lmna*^{N195K/N195K} MEFs in comparison to *Lmna*^{+/+} MEFs (wild-type controls)*

Image J analysis of acquired images for the immunofluorescence staining of PFA fixed cells using Hic-5 antibody indicates that there is no significant difference in steady state Hic-5 protein expression between the two mutant MEF cell lines and the WT control MEF cell line under baseline tissue culture conditions (Figure 9); a set of

representative images are shown in Figure 10 (lower panel). In comparison to control, an insignificant 1.11 - and 1.13 - fold change (± 0.11 , and ± 0.05) in relative fluorescence intensity of Hic-5 was noted in Lamin A/C null MEFs and in *Lmna*^{N195K/N195K} MEFs respectively ($P > 0.05$ for both). Results represent mean fold change \pm SEM of three independent experiments. Using Image J software, at least 50 cells per cell line from different image frames per experiment amounting to an average total of 150 cells per cell line were analyzed. Furthermore, we did not notice a difference in the intracellular distribution of immuno-stained cavolin-1 α between the three cell lines. However, there seems to be a difference in the intracellular distribution of immuno-stained Hic-5 in the two mutant lines (more cytoplasmic to nuclear signal) in comparison to WT, but this requires further validation.

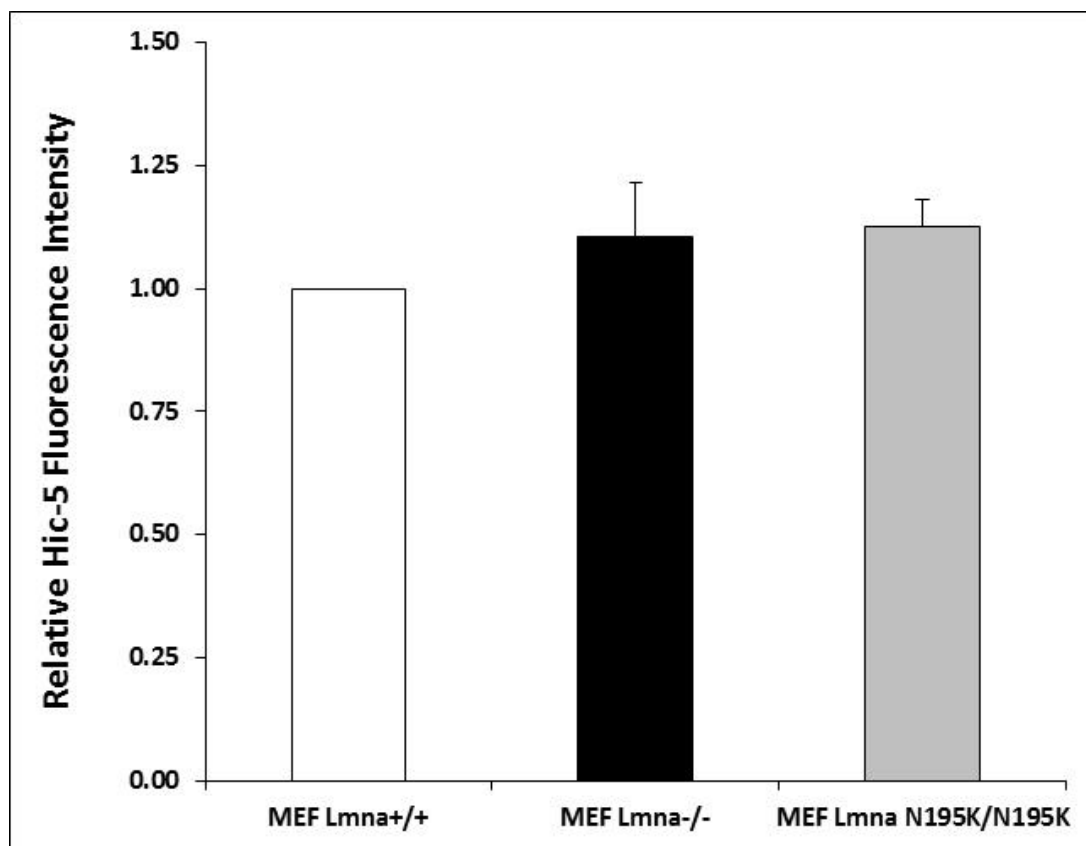


Figure 9: a semi-quantitative assessment of the relative fluorescence intensity of Hic-5 immunostaining in *Lmna*^{-/-} and in *Lmna*^{N195K/N195K} MEF cells in comparison to WT control MEF cells at baseline conditions shows no significant difference in expression between the three cell lines. Data represent mean ± SEM derived from 3 independent experiments. An average total of 150 cells per cell line were analyzed using image J software.

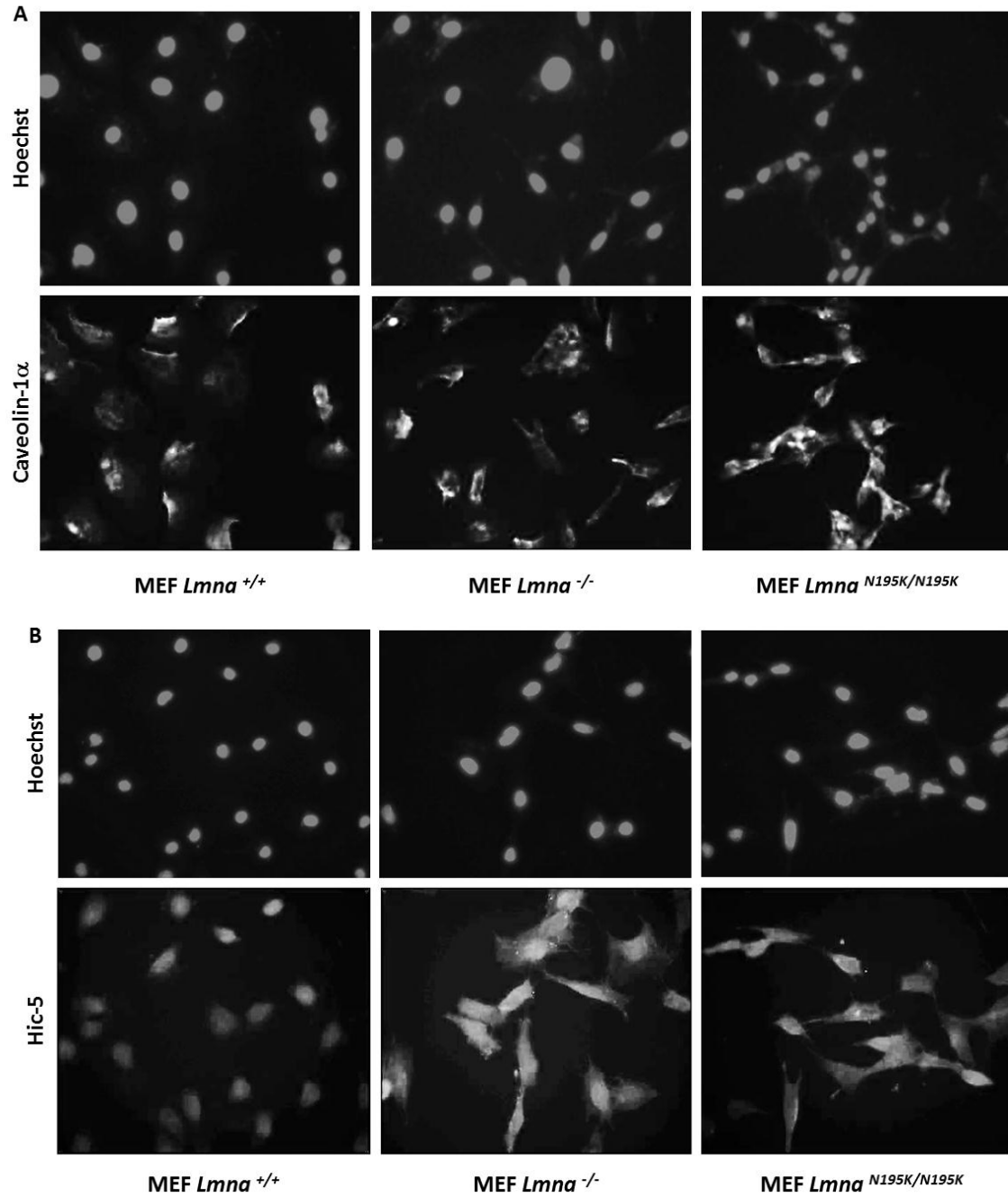
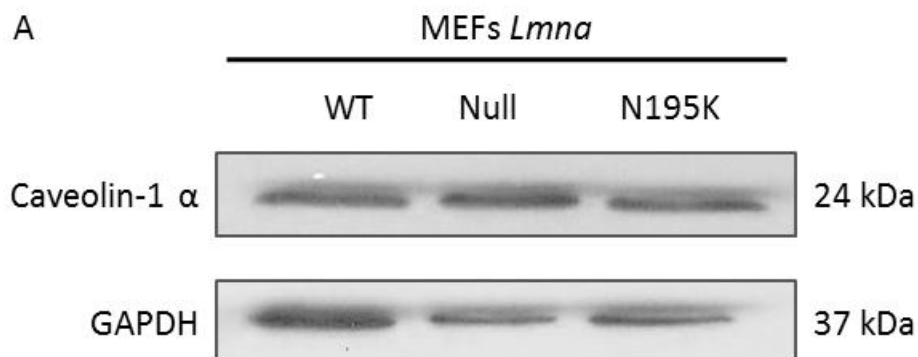


Figure 10: representative images (40x, magnification) showing immunofluorescence staining of Cav-1 α (A; lower panel) and Hic-5 (B; lower panel) in MEF cells deficient in A-type lamins and in MEF cells expressing the N195K mutant form in comparison to MEF cells expressing WT Lamin A/C. Hoechst was used for nuclear staining (A, B; upper panels).

2.3 Western Blot analysis of caveolin-1 α shows no significant difference in steady state protein expression levels in *Lmna*^{-/-} MEFs (Lamin A/C null) and in *Lmna*^{N195K/N195K} MEFs in comparison to *Lmna*^{+/+} MEFs (wild-type controls)

We aimed to assess the expression levels of Cav-1 α protein at baseline conditions in *Lmna* null MEFs (*Lmna*^{-/-}) and in *Lmna*^{N195K/N195K} MEFs in comparison to WT control cells by Western Blot analysis of total protein extracts from cell lysates using a Cav-1 α specific antibody. Qualitative analysis was done by observing and comparing densitometry signals on autoradiography film between the various samples. Then, semi-quantitative densitometry analysis was done using Image J software. Our results show that under baseline conditions there is no significant difference in Cav-1 α protein expression between the two mutant cell lines and the control (Figure 11). A 1.16 - fold change (± 0.23) in Cav-1 α protein expression in *Lmna* null MEFs was not significantly different compared to the *Lmna* WT MEF controls ($P > 0.05$). Likewise, an insignificant 1.09 - fold (± 0.14) change in Cav-1 α protein expression was obtained in *Lmna*^{N195K/N195K} MEFs compared to the control ($P > 0.05$). Results represent mean fold change \pm SEM of three independent experiments.



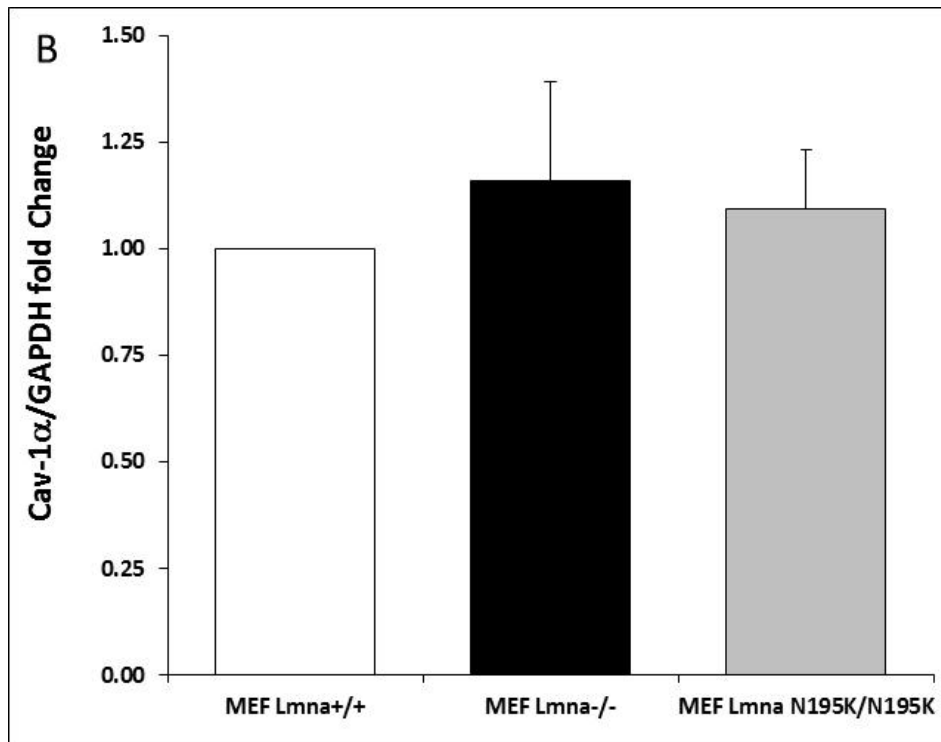


Figure 11: Western Blot analysis of Cav-1 α protein expression in $Lmna^{-/-}$ and in $Lmna^{N195K/N195K}$ MEF cells vs. control WT cells at baseline conditions (A; representative blot). Image J analysis of the Cav-1 α densitometry signal normalized to that of the GAPDH loading controls shows no significant difference in Cav-1 α protein expression between the two mutant cell lines and the WT control. Data represent mean fold change \pm SEM derived from 3 independent experiments

2.4 Western Blot analysis of Hic-5 protein expression suggests a differential

expression of Hic-5 isoforms in $Lmna^{N195K/N195K}$ MEFs in comparison to $Lmna$ null MEFs ($Lmna^{-/-}$) and $Lmna^{+/+}$ MEFs (wild-type controls).

We also studied Hic-5 expression in the two mutant cell lines versus the control WT cell line by Western Blot analysis. Under the experimental conditions we used, we were able to detect three Hic-5 isoforms ranging in size between 49 and 55kDa. Our data suggest that there is a differential expression of the three Hic-5 isoforms between the three

cell lines; most notable in the N195K mutant cells in that we noted decreased levels for all three isoforms in comparison to the WT control cells (Figure 12 A). On the other hand, there seems to be an increased expression of all three isoforms in the *Lmna null* MEFs (*Lmna*^{-/-}) in comparison to WT controls. Image J analysis of the Hic-5 densitometry signal (collectively measured for all three isoforms) normalized to that of the GAPDH loading control suggests that there is an estimated 1.5 – fold increase in Hic-5 expression (of the three isoforms pooled together) in *Lmna null* MEFs compared to WT controls (Figure 12B). On the other hand, Hic-5 expression in *Lmna*^{N195K/N195K} MEF cells decreased by an estimated 0.71- fold compared to WT controls. However, the decrease observed in Hic-5 protein expression in *Lmna*^{N195K/N195K} MEFs is not equivalent for all three isoforms. Our data suggest that the 51kDa isoform is nearly not expressed at all in this cell line or is below the detection limit of this assay. There also seems to be a differential expression of the three isoforms between *Lmna*^{N195K/N195K} MEFs and *Lmna null* MEFs. Results represent the average of two independent experiments; four independent Western Blot analysis experiments were performed to validate these results, but we could quantify densitometry for only two of these assays due to low quality resolution in the densitometry signals obtained in two of the assays likely resultant from high background and the use of a different type of autoradiography films which had less sensitivity and lower resolution quality.

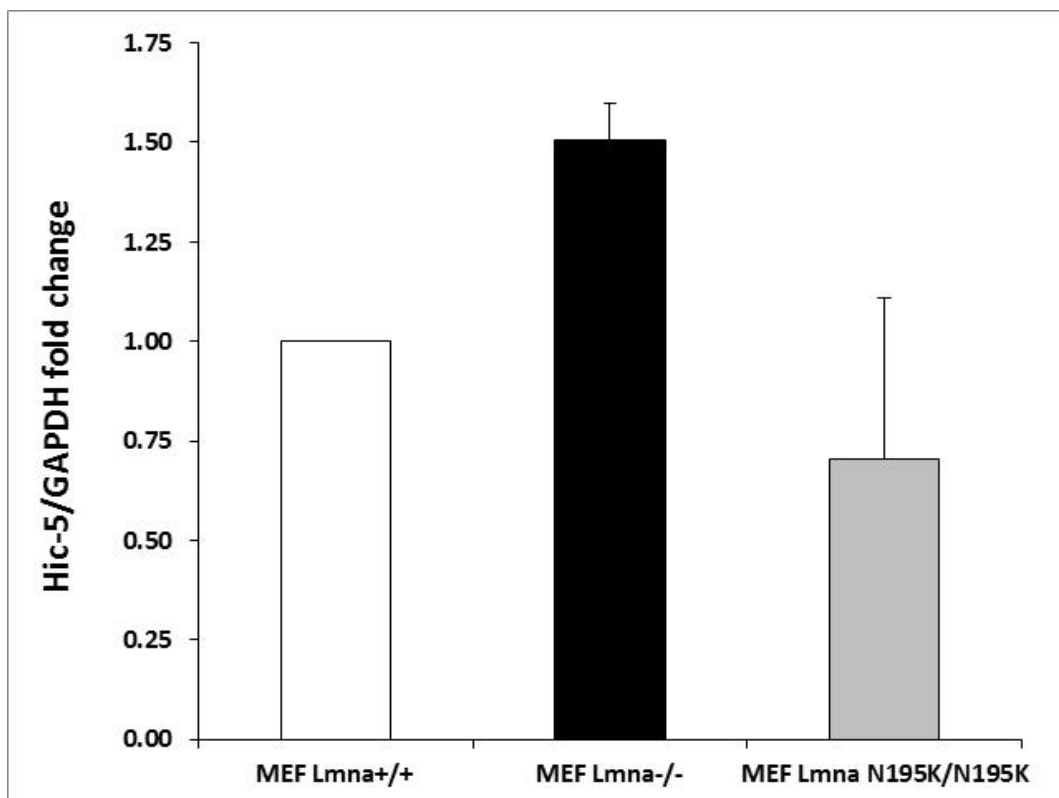
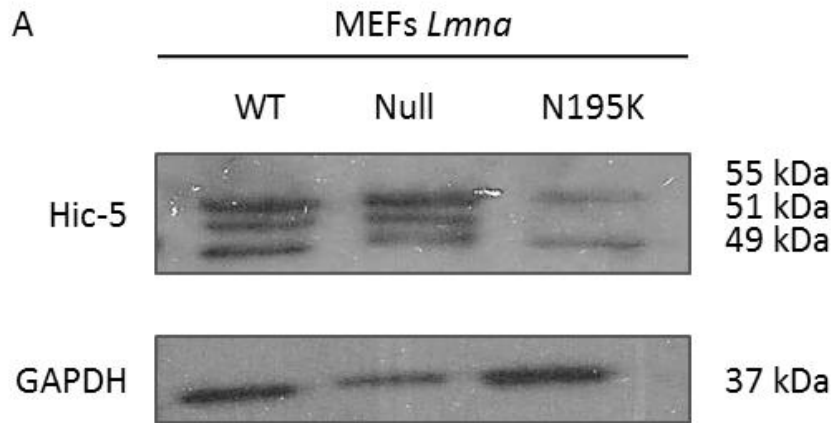


Figure 12: Western blot analysis of Hic-5 protein expression in *Lmna*^{-/-} and in *Lmna*^{N195K/N195K} MEF cells vs. control WT cells at baseline conditions (A; representative blot). Image J analysis of the Hic-5 densitometry signal (collectively measured for three isoforms) normalized to the GAPDH loading control suggests an increase in Hic-5 protein expression in *Lmna*^{-/-} MEFs and a decrease in *Lmna*^{N195K/N195K} MEF cells compared to the control. In addition, there seems to be a differential expression of these isoforms between the three cell lines. Data represent mean fold + Standard Deviation (STDEV) change from 2 independent experiments.

Aim 3: to investigate the effect of oxidative stress on the expression profile of *Cav-1* and *Hic-5* in MEFs derived from mouse models of EDMD and DCM in comparison to wild-type controls

3.1 Optimization of H₂O₂ Exposure Parameters

In order to assess the response of *Lmna* null (*Lmna*^{-/-}) and *Lmna*^{N195K/N195K} MEF cells to oxidative stress, cells were exposed to sub-apoptotic concentrations of hydrogen peroxide (H₂O₂) for specific time points after which RNA was extracted. To do so, we had to test for the appropriate concentrations and exposure time points that would cause stress to the cells, but not cause them to undergo apoptosis. We used *Lmna* WT MEFs for parameter optimization since they represent control cells with normal function. It is known that when exposed to stress, cells undergo morphological changes, by changing into a round up morphology followed by appearance of cell membrane blebs. These are detectable by microscopic observation. When cells undergo apoptosis, they float. Based on that, we decided to test for the appropriate concentration by exposing cells to a range of H₂O₂ concentrations followed by microscopic observation in comparison to control untreated cells. We chose the first set of concentrations after mining the literature. The first trial was setup by exposing cells to 5 different concentrations of H₂O₂, these were: 1.0, 5.0, 10.0, 50.0, and 100.0 μM for 2, 4, and 6 hours (conditions and observations are summarized in Table 3). All cells exposed to concentrations above 1.0 μM for 2 hours detached and floated in the media shortly afterwards whereas the cell population that was exposed to 1.0 μMH₂O₂ for 2 hours was similar in morphology and adherence characteristics to the control cells that were mock treated with the exception of the observation of a few cells showing minor changes in cellular shape and size. After 4

hours of exposure, almost all of the cells treated with 1.0 μM H_2O_2 exhibited changes in cell morphology as compared to the mock control. After 6 hours of exposure to 1.0 μM H_2O_2 , some floaters started to appear in the media.

Table 3: a summary of the experimental parameters and the cell morphology observations made of the *Lmna*^{+/+} MEF cells in response to varying concentrations of H_2O_2 after 2hr of exposure

| Cell morphology at 2hr / H_2O_2 Concentration (μM) | Normal | Stressed | Surface Blebs | Detached |
|--|--------|----------|------------------|----------|
| 100.0 | | ✓ | ✓ | ✓ |
| 50.0 | | ✓ | ✓ | ✓ |
| 25.0 | | ✓ | ✓ | ✓ |
| 5.0 | | ✓ | ✓ | ✓ |
| 1.0 | ✓ | | | |

In the second trial, we scaled down the experimental parameters to include 0.10, 0.25, 0.50, 0.75, and 1.00 μM of H_2O_2 with exposure time points of 2 hours and 4 hours (conditions and observations are summarized in Table 4). Cells exposed to 1.00 and 0.75 μM of H_2O_2 showed minor changes in morphology after 2 hours of exposure. A smaller number of cells showed a similar change in morphology when exposed to 0.50 μM . On the other hand, cells exposed to the remaining 2 concentrations had similar morphological and adherence characteristics as the mock treated control cells after 2 hours of exposure. At 4 hours, cells exposed to 1.00 and 0.75 μM H_2O_2 had a drastic change in morphology as compared to the control; cells exposed to 0.50 μM H_2O_2 also exhibited a marked change in morphology whereas cells exposed to 0.25 μM and 0.10 μM did not exhibit any change in morphology. At 6 hours, cells exposed to 1.00 and

0.75 μM were completely detached and floating in the media. Cells exposed to 0.50 μM H_2O_2 also showed a considerable amount of floaters compared to the control; those treated with 0.25 and 0.10 μM showed no significant change in morphology.

Table 4: a summary of the experimental parameters and the cell morphology observations made of the *Lmna*^{+/+} MEF cells in response to varying concentrations of H_2O_2 after 4hr of exposure

| Cell morphology at 4hr / H_2O_2 Concentration (μM) | Normal | Stressed | Surface Blebs | Detached |
|---|--------|----------|---------------|----------|
| 1.00 | | ✓ | ✓ | |
| 0.75 | | ✓ | ✓ | |
| 0.50 | | ✓ | | |
| 0.25 | ✓ | | | |
| 0.10 | ✓ | | | |

In the third trial, we observed the cellular morphological changes of *Lmna* null (*Lmna*^{-/-}) and *Lmna*^{N195K/N195K} MEF cells in response to 0.1, 0.25, and 0.5 μM of H_2O_2 following 2, 4, and 6 hours of exposure (conditions and observations are summarized in Table 5). At 2 hours, both mutant cell lines showed minor changes in cell morphology and adherence characteristics in comparison to mock treated controls when exposed to 0.5 μM H_2O_2 , whereas cells exposed to 0.10 and 0.25 μM H_2O_2 exhibited no change on morphology compared to mock controls. At 4 hours, both mutant cell lines showed signs of stress when exposed to either concentration and at 6 hours, massive apoptosis was observed in cells exposed to 0.25 and 0.5 μM , whereas a marked change in morphology accompanied with some detachment was noted in cells that were exposed to 0.10 μM H_2O_2 .

Table 5: a summary of the experimental parameters and the cell morphology observations made of the *Lmna*^{-/-} and the *Lmna*^{N195K/N195K} MEF cells in response to varying concentrations of H₂O₂ after 2hr of exposure

| Cell morphology at 2hr / H ₂ O ₂ Concentration (μM) | Normal | Stressed | Surface Blebs | Detached |
|---|--------|----------|---------------|----------|
| 0.50 | | ✓ | | |
| 0.25 | ✓ | | | |
| 0.10 | ✓ | | | |

Considering that our aim is to investigate the effect of H₂O₂ – induced oxidative stress on the expression profile of *Cav-1* and *Hic-5* in the two mutant MEF cell lines in comparison to wild-type controls, we are interested in H₂O₂ concentrations that induce stress, but do not cause apoptosis and cell detachment. Accordingly, and based on the observations made during parameter optimization trial experiments, we decided to select the 0.10 and 0.50 μM H₂O₂ concentrations (5 - fold difference between the two) and four immediate - early time points (5, 15, 30, 60 min) for further experiments whereby cells would be exposed, RNA would be extracted, and reverse transcribed, then *Cav-1α* and *Hic-5* H₂O₂ - induced expression would be quantified using Real-Time PCR. We report in this thesis the *Hic-5* data only.

3.2 The response of *Lmna* null (*Lmna*^{-/-}) and *Lmna*^{N195K/N195K} MEF cells to oxidative stress induced by hydrogen peroxide compared to WT cells suggests a differential gene expression pattern for *Hic-5* between the three cell lines

In order to assess the *Hic-5* response of *Lmna* null (*Lmna*^{-/-}) and *Lmna*^{N195K/N195K} MEF cells to H₂O₂ - induced oxidative stress, all three cell lines were exposed to 0.1 and

0.5 μM of H_2O_2 for varying time points (5, 15, 30, and 60 min), followed by RNA extraction, reverse transcription, and quantification of *Hic-5* gene expression by Real-Time PCR. All results represent mean fold change \pm SEM derived from 3 independent experiments, each performed in duplicates.

At 5 minutes, in wild - type *Lmna* MEF cells, we obtained a 2.32 - and 2.66 - fold (± 0.64 and ± 0.89) increase in the expression levels of *Hic-5* in response to 0.50 and 0.10 μM of H_2O_2 respectively, but this was not statistically significantly different from the mock treated wild - type controls ($P > 0.05$ for both values). At 15 min, the levels of *Hic-5* transcript dropped to 1.59 - and 1.46 - fold (± 0.45 and ± 0.29) change in response to 0.50 and 0.10 μM H_2O_2 respectively (Figure 13). Likewise, this change was not statistically significantly different from the mock treated wild - type controls ($P > 0.05$ for both values). At 30min, *Hic-5* gene expression in *Lmna* WT MEFs decreased to 0.90 - and 0.65 - fold (± 0.18 and ± 0.22) in comparison to mock treated control cells in response to 0.50 and 0.10 μM H_2O_2 respectively. At 1 hour following exposure to 0.50 and 0.10 μM H_2O_2 respectively, the expression of *Hic-5* seemingly normalizes with 1.08 - and 0.96 - fold change (± 0.27 and ± 0.21) which are not statistically different from the mock treated control cells ($P > 0.05$ for both values).

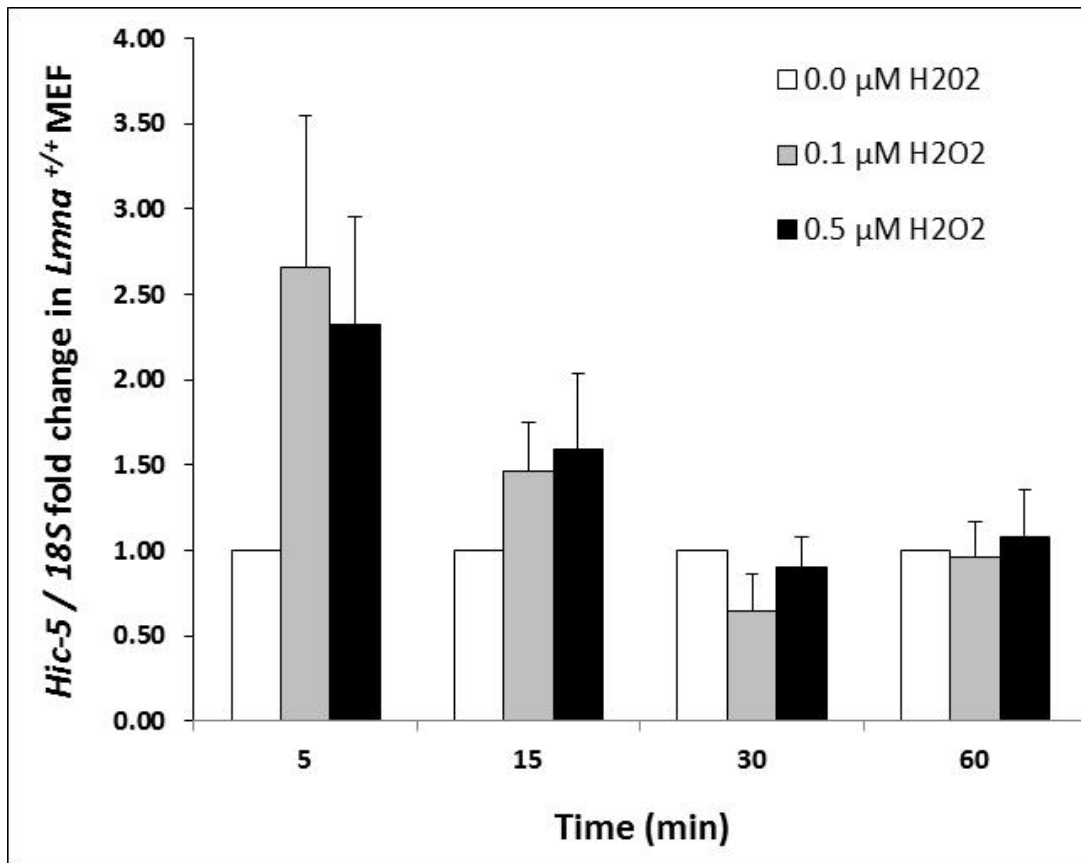


Figure 13: *Hic-5* immediate – early transcript expression normalized to that of *18S* reference gene in *Lmna* WT MEF cells following exposure to 0.1 and 0.5 μM of H_2O_2 at 4 different time points. Cells respond quickly. A marked increase in *Hic-5* gene expression was measured as quickly as 5 minutes post exposure to both concentrations. *Hic-5* transcript levels drop afterwards to reach whereby minimal expression was measured 30 minutes post exposure to both H_2O_2 concentrations. *Hic-5* transcript levels reach baseline levels in comparison to those of the mock treated control cells at 1 hour post exposure. Data represent mean fold change \pm SEM derived from 3 independent experiments, each performed in duplicates.

The response of *Lmna* null (*Lmna*^{-/-}) MEF cells was less pronounced at 5 minutes as the transcript levels of *Hic-5* showed an insignificant decrease of 0.80 - and 0.77 - fold (\pm 0.12 and \pm 0.19) post treatment with 0.5 and 0.1 μM H_2O_2 respectively ($P > 0.05$ for both values). These levels remained steady at 15 minutes whereas the response peaked with a 1.47 - fold increase (\pm 0.52) in *Hic-5* expression at 30 min post treatment with 0.5 μM H_2O_2 (Figure 14). However, this increase in expression was not statistically

significantly different from that measured following treatment with 0.1 μM H_2O_2 . The expression then significantly drops to 0.62 - fold change (± 0.01) at 1hour post treatment with 0.5 μM H_2O_2 ($P= 0.0001$), and it bounces to near baseline levels with a 1.00- fold change (± 0.33) following treatment with 0.1 μM H_2O_2 .

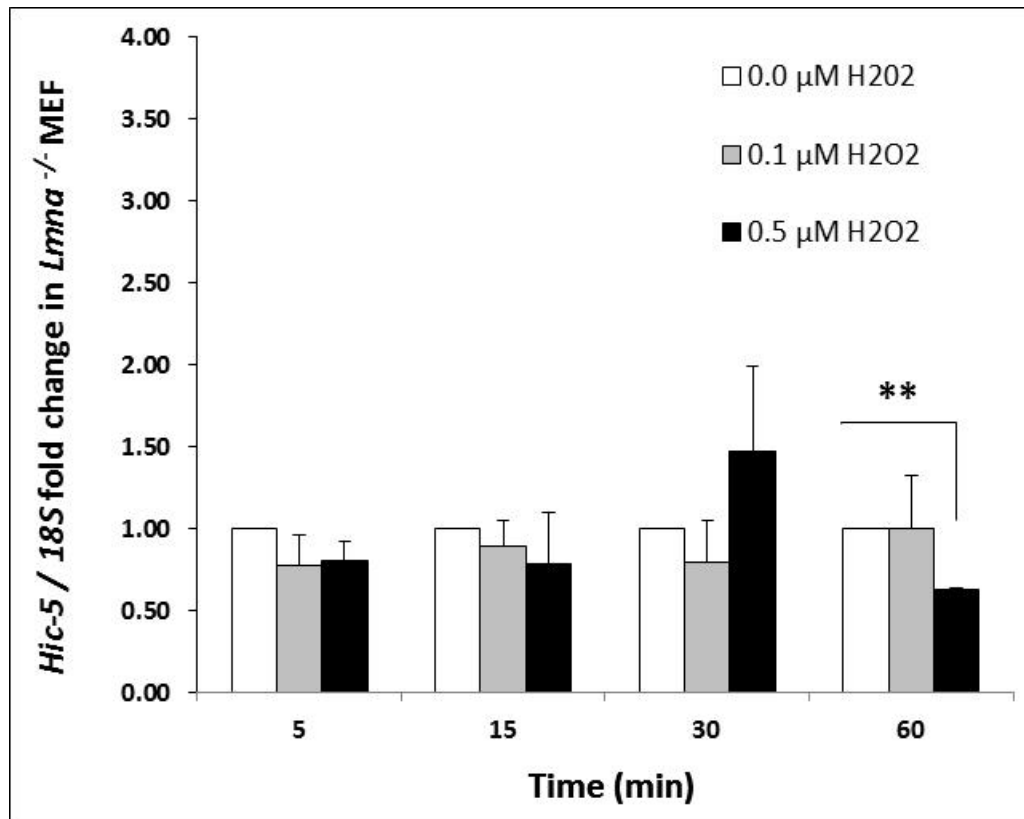


Figure 14: *Hic-5* immediate – early transcript expression normalized to that of *18S* reference gene in *Lmna* null MEF cells following exposure to 0.1 and 0.5 μM of H_2O_2 at 4 different time points. A delay in response to hydrogen peroxide exposure was noticed as compared to that in *Lmna* wild - type control MEF cells. A marked increase in *Hic-5* gene expression was measured at 30 minutes post exposure to 0.5 μM of H_2O_2 . *Hic-5* transcript levels post treatment with 0.1 μM of H_2O_2 reach baseline levels in comparison to those of the mock treated control cells at 1 hour post exposure. Data represent mean fold change \pm SEM derived from 3 independent experiments, each performed in duplicates. Asterisks represents statistical significance ($p<0.01$).

In *Lmna*^{N195K/N195K}MEF cells, the maximum *Hic-5* gene induction response was noted at 15 minutes following treatment with 0.5 and 0.1 μM H_2O_2 in that a 1.91 - and a 2.34 - fold (± 1.14 and ± 0.85) increase in *Hic-5* transcript expression was measured respectively (Figure 15). However, this marked increase was not statistically significantly different from that of mock treated control cells due to the large standard deviation in the obtained results ($P > 0.05$ for both values). After the peak expression that was reached at 15 minutes, *Hic-5* transcript levels drop to 1.35 - and 1.90 - fold (± 0.29 and ± 0.79) in comparison to transcript levels of the mock treated control cells quantified at 30 minutes following treatment with 0.5 and 0.1 μM H_2O_2 respectively. *Hic-5* transcript expression leveled down to 0.81 - and 0.56 - fold (± 0.23 and ± 0.26) that of the mock controls at 1 hour post exposure to both H_2O_2 concentrations respectively

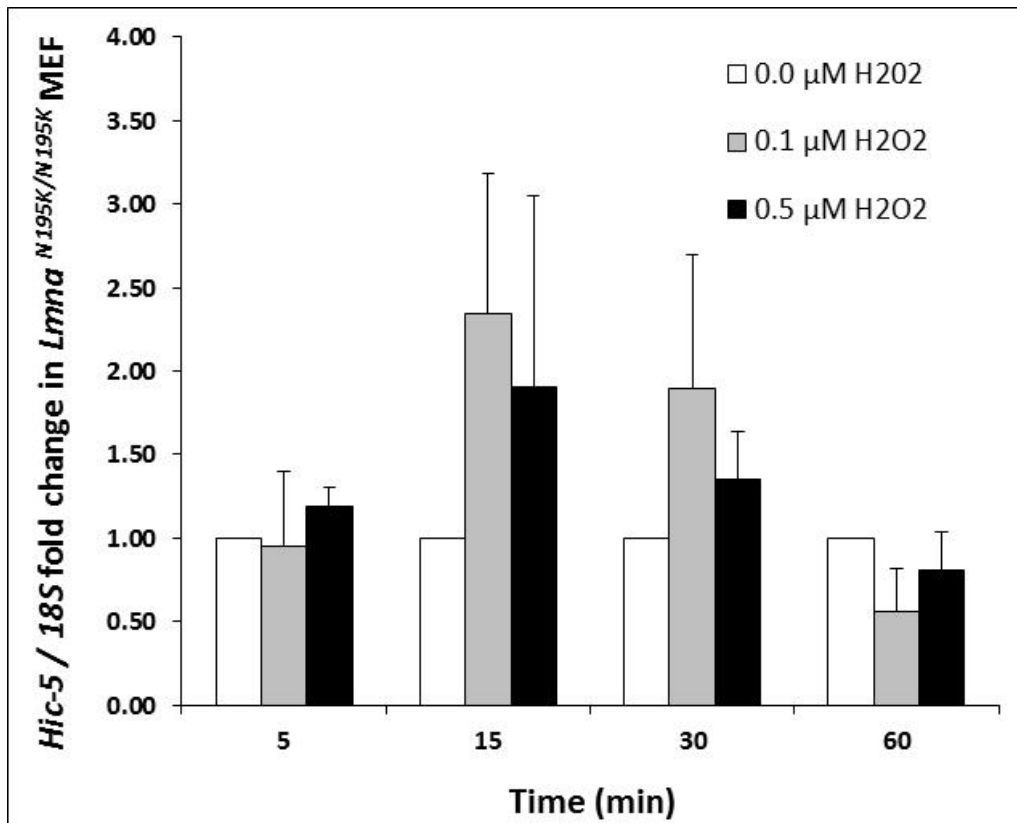


Figure 15: *Hic-5* immediate – early transcript expression normalized to that of *18S* reference gene in *Lmna* N195K mutant MEF cells following exposure to 0.1 and 0.5 μM of H_2O_2 at 4 different time points. A delay in response to hydrogen peroxide exposure was noticed as compared to that in *Lmna* wild - type control MEF cells. A marked increase in *Hic-5* gene expression was measured at 30 minutes post exposure to 0.1 and 0.5 μM of H_2O_2 . *Hic-5* transcript levels go down below baseline levels in comparison to those of the mock treated control cells at 1 hour post exposure. Data represent mean fold change \pm SEM derived from 3 independent experiments, each performed in duplicates.

CHAPTER IV

DISCUSSION

Laminopathies refer to a group of diseases that affect a range of tissues in the body. To date the molecular mechanisms that explain how mutations in a single ubiquitous gene are manifested in a tissue specific manner have not been deciphered yet. A number of hypotheses have been proposed of which two have stood out the most; these are the “gene regulation” hypothesis and the “structural hypothesis”. The gene regulation theory proposes that perturbed gene regulation is behind the phenotypic diversity observed in laminopathies and is of interest to us, especially that evidence showed multiple interactions between lamin A/C and a number of key regulators of cellular functions. These include transcription factors and other interacting partners that function in a tissue specific manner. Our interest to study select mechanosensitive genes (*CAV-1* and *Hic-5*) in relation to the gene regulation theory stems out from the fact that both EDMD and DCM are manifested in tissues subjected to mechanical stress. Accordingly, we hypothesized that alterations in the expression profile of these genes and their corresponding proteins may contribute to the pathogenesis, or at the least may exist, in muscular laminopathies. Our data show that *Cav-1* alpha expression is significantly down regulated by 0.51 – fold in *Lmna*^{N195K/N195K} MEFs in comparison to wild-type controls and its borderline significantly changed by 0.48 - fold in *Lmna*^{-/-} MEFs. Cav-1 alpha has long been studied not only in the context of caveolae. In fact, Sotgia *et al.* 2012 showed that the levels of Cav-1 alpha are elevated in normal tissues where they act as negative regulators of proliferation. Moreover, caveolin null MEFs show a hyper-proliferative phenotype. The fact that fibroblasts lacking functional A –

type lamins show increased proliferation (Johnson *et al.*, 2004; Van Berlo *et al.*, 2005; Ivorra *et al.*, 2006; Nitta *et al.*, 2006) may thus be linked to this down-regulation, in part explaining the increased proliferation rate observed in the *Lmna*^{N195K/N195K} and in *Lmna*^{-/-}MEF cells. The role of Cav-1 alpha in cellular proliferation is attributed to its function in cholesterol enriched membrane micro domains (CEMM) to which signaling molecules are targeted via integrin signaling. These signaling molecules including Rho GTPases activate a cascade of downstream events among which is the activation of pRb, which is known to interact with lamin A/C protein, controlling the cell cycle progression. pRb regulation hence seems to cross link both pathways.

Next, we assessed the expression of Cav-1 alpha at the protein level by two distinct methods. We took into consideration the fact that Cav-1 protein is a lipid raft protein and its expression is very much affected by cell-cell contact and density of cells in tissue culture. Thus, and to account for that, we decided to study the expression of Cav-1 alpha not only by Western Blot analysis, but also by immune-fluorescence staining. When assessing the expression by IF, we could make sure that the cell spreading and confluence of cells is similar across the three cell lines and across the different independent repeats. It also enabled us to assess whether there is a differential distribution of Cav-1 alpha protein in the two mutant cell lines versus the control. Our data suggest that the overall expression of Cav-1 alpha is not significantly perturbed in *Lmna*^{N195K/N195K}MEFs, and in *Lmna*^{-/-}MEFs in comparison to wild-type controls as indicated by a 1.14 - and 1.03- fold difference respectively following semi quantitative assessment. In addition, the overall distribution of the protein seems to be similar across all three cell lines. A number of studies show that Cav-1 alpha exists in multiple forms one of which is secreted into the medium. The fact that we could see a down-regulation

of *Cav-1* alpha at the transcriptional level and not at the protein level suggests that both *Lmna*^{N195K/N195K} MEFs and *Lmna*^{-/-} MEFs might compensate for the decreased gene expression by retaining Cav-1 alpha in the cell and decreasing its rate of secretion. This can be studied by analyzing the secreted protein fraction of the cells and assessing the abundance of Cav-1 alpha relative to control. Another factor that could explain, at least in part, the results we have obtained is that the half-life, and consequently the turnover rate, of Cav-1 alpha might differ in the two mutant cell lines versus wild-type control; i.e. the decreased transcriptional levels of *Cav-1* alpha as might be counterbalanced by a delay its breakdown at the protein level in both mutant lines in comparison to WT control cells. Considering that Cav-1 exists in two isoforms (alpha and beta) and taking into account the differential roles played by these two isoforms during development, our next step would be to study the total Cav-1 pool at the transcriptional level and at the translational level. Any change in the total Cav-1 pool would reflect that of Cav-1 beta isoform. Knowing that patients suffering from muscular laminopathies show a perturbed cytoskeletal dynamics on one hand, and that Cav-1 isoforms interact differentially with cytoskeletal elements, especially actin, our ongoing study would be the first to assess the differential role played by both isoforms in particular in the context of muscular laminopathies and it may well provide an in depth mechanistic insight into the disease pathogenesis. Our future aims would also include studying the effects of stress, be it mechanical or oxidative-induced, on the expression of Cav-1(alpha and beta) both at the transcriptional and translational level. As mentioned before, patients suffering from laminopathies exhibit higher ROS species; thus are more susceptible to oxidative stress. Additionally, it would be interesting to check whether or not the phosphorylated state of Cav-1 alpha is differentially regulated following induction of stress in the two mutant

cell lines versus the control. It is known that this post translational modification of the protein happens in response to oxidative stress and is required for the proper functioning of Cav-1 alpha isoform. Our pilot study, hence, provides for the first time some clues about the putative role of caveolin-1 alpha in muscular laminopathies. It remains crucial to further investigate the mechanisms by which alterations in caveolin-1 signaling contribute to the progression of the disease. Knowing that the laminopathies we are investigating are those affecting muscle tissue, it also remains imperative to investigate the expression of other caveolin isoforms especially caveolin-3, being the isoform exclusively expressed in muscle cells. Any finding in this regard, will have to be further validated in cardiac myocytes, C2C12 myoblasts *in vitro*, and later in skeletal and cardiac muscle tissue sections derived from disease mice models; to this end, *in vivo* validation of the results should follow. Ultimately, this will help to provide insight to the mechanisms of muscular laminopathies in a more relevant context.

Hic-5, also known as hydrogen peroxide inducible clone5, is another gene we decided to study in relation to muscular laminopathies. Since both mutant cell lines under investigation were derived from mouse models of muscular dystrophy (patients suffer from muscle degeneration and impaired muscle regeneration) and knowing that several studies point out to the central role of *Hic-5* in myogenesis, we hypothesized that *Hic-5* expression, both at the transcriptional and translational level, might be deregulated in *Lmna*^{-/-} and *Lmna*^{N195K/N195K} MEF cells at baseline in comparison to wild-type controls. Our data suggest an up-regulation in the expression of *Hic-5* at the transcriptional level whereby a 1.95 – and a 1.75 – fold increase was measured in *Lmna*^{N195K/N195K} and *Lmna*^{-/-} MEF cells respectively. Previous studies show that *Hic-5* induces senescence - like phenotype in immortalized human fibroblast (Shibanuma *et*

al., 1997). The increased levels of *Hic-5* may thus explain in part the impaired muscle regeneration observed in the studied disease models. In a study published by Gao *et al* in 2005, it was shown that the expression of *Hic-5* isoforms is spatially and temporally regulated and that understanding the full scope of *Hic-5* isoforms differential functions should involve a careful approach; i.e. due to the contradictory data from different labs in terms of their biological function especially during myogenesis in that some reports were in favor for *Hic-5* role in inducing myogenesis and other studies reported that *Hic-5* as implicated in inhibition of myogenesis (Shibanuma *et al.*, 2002) and (Hu *et al.*, 1999). Our study however, was limited to murine fibroblasts in culture. As such, for a better assessment of the role of *Hic-5* in muscular laminopathies, its expression is to be assessed in cardiac myocytes, in C2C12 myoblasts, and in skeletal and cardiac muscle tissue sections derived from diseased mouse models, which we aim to conduct as part of our future aims. In addition, knowing that *Hic-5* isoforms are differentially expressed among tissues (Gao *et al.*, 2005), we suspect that certain isoforms might be more involved in muscle cell biology than others and are differentially expressed among the different cell lines. This hypothesis stems out from our observation of *Hic-5* expression at the protein level in Western Blot analysis performed on total protein extracts from cell lysates derived from the three tested cell lines. We could clearly detect 3 isoforms of *Hic-5* and it seems that the three are down-regulated in *Lmna*^{N195K/N195K} MEF cells at the protein level, but to our surprise this was not the case for *Lmna* null MEFs. Not only does that suggest that *Hic-5* expression might be deregulated in certain muscular laminopathy models, but also that this deregulation differs between the different types of muscular laminopathies. It would suggest a differential role played by specific isoforms in particular in DCM and not in EDMD. This would be the first attempt to

study the expression of *Hic-5* in such a context; more so the differential expression of isoforms within the same class of muscular laminopathies. It remains to be determined as to what this deregulation means at the mechanistic level and whether it provides insight to possible differences that may contribute to the disease pathogenesis in the various muscular laminopathies.

We also assessed the protein expression of *Hic-5* through immune-fluorescence staining. Our data suggest that there is no significant difference in the total *Hic-5* content between *Lmna*^{N195K/N195K} MEFs and *Lmna* null MEFs on one hand and the wild - type control cells on the other. The increase in *Hic-5* expression at the transcriptional level in *Lmna*^{N195K/N195K} MEFs and in *Lmna* null MEFs on one hand and the stable *Hic-5* protein content on the other, might suggest that the turnover rate of *Hic-5* in both mutant cell lines is higher than that in the control, meaning that the protein may be degraded at a much faster rate.

Since *Hic-5* is known to be induced by oxidative stress, we aimed to study the induction in *Hic-5* transcript expression in response to hydrogen peroxide in *Lmna*^{N195K/N195K} MEFs and in *Lmna* null MEFs and compare the pattern we obtain to that of wild - type MEFs. We hypothesized that the response of the two mutant cell lines is different than that of the wild – type cells, given that the data we got at baseline conditions suggested a higher pool of *Hic-5* transcripts upfront in comparison to the control. We studied the expression profile of *Hic-5* at 4 different time points: 5, 15, 30, and 60 minutes following exposure to 2 concentrations of H₂O₂ (0.1 and 0.5 μM). The compiled data served to give us an idea about *Hic-5* expression across a time line. Our data show that wild - type MEF cells respond faster to H₂O₂ induction with a peak response of 2.33 - and 2.66 - fold change post treatment with 0.5 and 0.1 μM H₂O₂

respectively which was measured after 5 minutes of induction in comparison to a delayed response in both *Lmna* null and *Lmna*^{N195K/N195K} MEF cells. In fact, we suspect that the *Lmna* null and *Lmna*^{N195K/N195K} MEF cells may rely on the elevated levels of *Hic-5* transcripts upfront at baseline condition to generate the needed *Hic-5* protein post stress induction which may in part explain the delayed response in *Hic-5* induction post H₂O₂. In *Lmna* null MEF cells, the normal level of 1- fold was restored at 1 hour post treatment with 0.1μM of hydrogen peroxide whereas it was maintained below 1-fold at 5, 15 and 30 minutes which might indicate that the cell had enough levels of *Hic-5* transcript upfront prior to oxidative stress induction. In *Lmna*^{N195K/N195K} MEF cells, a peak response was delayed however not to the same extent as that of the *Lmna* null MEF cells; it was measured at 15 minutes following treatment with both H₂O₂ concentrations. Further investigation of the differential profiles that were observed in *Hic-5* induction post H₂O₂- induced oxidative stress in the two mutant cell lines might provide new insights into the putative role *Hic-5* may play in the disease pathogenesis in both DCM and EDMD.

Another interesting observation regarding *Hic-5* function is its shuttling between focal adhesions and the nucleus upon oxidative stress via oxidant sensitive nuclear export signals that regulate its nuclear accumulation (Shibanuma *et al.*, 2003) where it functions as a transcription factor regulating the expression of downstream genes. In this regard, it would be interesting to study the localization and intracellular distribution of *Hic-5* upon oxidative stress; we speculate that the shuttling of *Hic-5* between the two compartments might be impaired in the two mutant cell lines. This will have to be confirmed by immune-fluorescence staining post H₂O₂ induction and comparing the nuclear versus cytoplasmic distribution. As part of our future work plans, we aim to

assess Hic-5 expression in other forms of laminopathies affecting other tissues too. We hypothesize that Hic-5 is specifically deregulated in muscular laminopathies and not much in other types of laminopathies knowing the implication of Hic-5 in myogenesis.

Our study of Hic-5 expression under both baseline conditions and post H₂O₂-induced oxidative stress will have to be assessed in a more relevant context such as in cardiac myocytes, C2C12 myoblasts, and tissue sections derived from cardiac and skeletal muscle tissue from EDMD and DCM mouse models. We also intend to study the effects of mechanical stress on Hic-5 expression levels both at the transcriptional and translational level. It is known that the phosphorylation state of Hic-5 is induced by stress, hence we also aim to study the phosphorylated form of Hic-5 in context of laminopathies and whether or not this post translational modification is affected in the different laminopathy mutant cell lines and tissue.

Given that Hic-5 functions as a transcription factor and that numerous examples from the literature point out to a role of lamin A/C in gene regulation via regulating the activity of transcriptional factors, it would also be interesting to test whether Hic-5 and lamin A/C protein interact/associate directly or indirectly by performing co-immunoprecipitation assays. This would provide even more insight to the intricate relation between Hic-5, lamin A/C, and laminopathies and the function of Hic-5 in that context.

Finally, studying the effects of specific lamin A/C mutations on the differential expression of mechanosensitive genes such as *Cav-1* and *Hic-5* offers new clues into the molecular and the cell biology of muscular laminopathies via gaining a better insight into the putative mechanisms responsible for the phenotypic complexity of laminopathies.

REFERENCES

- Albinsson, S., Nordström, I., Swärd, K., & Hellstrand, P. (2008). Differential dependence of stretch and shear stress signaling on caveolin-1 in the vascular wall. *American Journal of Physiology-Cell Physiology*, 294(1), C271-C279.
- Bertrand, A. T., Chikhaoui, K., Ben Yaou, R., & Bonne, G. (2011). Laminopathies: One gene, several diseases. *Biologie Aujourd'Hui*, 205(3), 147-162.
- Bione, S., Maestrini, E., Rivella, S., Mancini, M., Regis, S., Romeo, G., & Toniolo, D. (1994). Identification of a novel X-linked gene responsible for emery-dreifuss muscular dystrophy. *Nature Genetics*, 8(4), 323-327.
- Bonne, G., Di Barletta, M. R., Varnous, S., Bécane, H. M., Hammouda, E. H., Merlini, L., Urtizberea, J. A. (1999). Mutations in the gene encoding lamin A/C cause autosomal dominant emery-dreifuss muscular dystrophy. *Nature Genetics*, 21(3), 285-288.
- Boscher, C., & Nabi, I. R. (2012). CAVEOLIN-1: Role in cell signaling. *Caveolins and Caveolae*, 29-50.
- Broers, J. L. V., Peeters, E. A. G., Kuijpers, H. J. H., Endert, J., Bouten, C. V. C., Oomens, C. W. J., Ramaekers, F. C. S. (2004). Decreased mechanical stiffness in LMNA^{-/-} cells is caused by defective nucleo-cytoskeletal integrity: Implications for the development of laminopathies. *Human Molecular Genetics*, 13(21), 2567-2580.
- Butin-Israeli, V., Adam, S. A., Goldman, A. E., & Goldman, R. D. (2012). Nuclear lamin functions and disease. *Trends in Genetics*
- Caltagarone, J., Hamilton, R. L., Murdoch, G., Jing, Z., DeFranco, D. B., & Bowser, R. (2010). Paxillin and hydrogen peroxide-inducible-clone 5 (hic-5) expression and distribution in control and Alzheimer disease hippocampus. *Journal of Neuropathology and Experimental Neurology*, 69(4), 356.
- Cao, H., & Hegele, R. A. (2000). Nuclear lamin A/C R482Q mutation in Canadian kindreds with Dunnigan-type familial partial lipodystrophy. *Human Molecular Genetics*, 9(1), 109-112.

- Cohen, A. W., Park, D. S., Woodman, S. E., Williams, T. M., Chandra, M., Shirani, J., Weiss, L. M. (2003). Caveolin-1 null mice develop cardiac hypertrophy with hyperactivation of p42/44 MAP kinase in cardiac fibroblasts. *American Journal of Physiology-Cell Physiology*, 284(2), C457-C474.
- David-Watine, B. (2011). Silencing nuclear pore protein tpr elicits a senescent-like phenotype in cancer cells. *PLoS One*, 6(7), e22423.
- De Sandre-Giovannoli, A., Chaouch, M., Kozlov, S., Vallat, J. M., Tazir, M., Kassouri, N., Stewart, C. L. (2002). Homozygous defects in *Lmna*, encoding lamin A/C Nuclear-Envelope proteins, cause autosomal recessive axonal neuropathy in human (Charcot-Marie-Tooth disorder type 2) and mouse. *Journal of the Peripheral Nervous System*, 7(3), 205-205.
- De Vos, W. H., Houben, F., Kamps, M., Malhas, A., Verheyen, F., Cox, J., Marcelis, C. L. M. (2011). Repetitive disruptions of the nuclear envelope invoke temporary loss of cellular compartmentalization in laminopathies. *Human Molecular Genetics*, 20(21), 4175-4186.
- Dechat, T., Adam, S. A., & Goldman, R. D. (2009). Nuclear lamins and chromatin: When structure meets function. *Advances in Enzyme Regulation*, 49(1), 157.
- Dechat, T., Adam, S. A., Taimen, P., Shimi, T., & Goldman, R. D. (2010). Nuclear lamins. *Cold Spring Harbor Perspectives in Biology*, 2(11)
- Dittmer, T. A., & Misteli, T. (2011). The lamin protein family. *Genome Biol*, 12(5), 222.
- Duncan, A. J., Bitner-Glindzicz, M., Meunier, B., Costello, H., Hargreaves, I. P., López, L. C., Hardy, J. (2009). A nonsense mutation in *COQ9* causes autosomal-recessive neonatal-onset primary coenzyme Q₁₀ deficiency: A potentially treatable form of mitochondrial disease. *The American Journal of Human Genetics*, 84(5), 558-566.
- Fabrini, R., Bocedi, A., Pallottini, V., Canuti, L., De Canio, M., Urbani, A., Giovanetti, A. (2010). Nuclear shield: A multi-enzyme task-force for nucleus protection. *PLoS One*, 5(12), e14125.
- Fang, P. K., Solomon, K. R., Zhuang, L., Qi, M., McKee, M., Freeman, M. R., & Yelick, P. C. (2006). Caveolin-1 α and-1 β perform nonredundant roles in early vertebrate development. *The American Journal of Pathology*, 169(6), 2209-2222.
- Fatkin, D., MacRae, C., Sasaki, T., Wolff, M. R., Porcu, M., Frenneaux, M., De Girolami, U. (1999). Missense mutations in the rod domain of the lamin A/C gene as causes of dilated cardiomyopathy and conduction-system disease. *New England Journal of Medicine*, 341(23), 1715-1724.

- Fatkin, D., Otway, R., & Richmond, Z. (2010). Genetics of dilated cardiomyopathy. *Heart Failure Clinics*, 6(2), 129.
- Folker, E. S., Östlund, C., Luxton, G. W. G., Worman, H. J., & Gundersen, G. G. (2011). Lamin A variants that cause striated muscle disease are defective in anchoring transmembrane actin-associated nuclear lines for nuclear movement. *Proceedings of the National Academy of Sciences*, 108(1), 131-136.
- Freund, A., Laberge, R. M., Demaria, M., & Campisi, J. (2012). Lamin B1 loss is a senescence-associated biomarker. *Molecular Biology of the Cell*, 23(11), 2066-2075.
- Galbiati, F., Razani, B., & Lisanti, M. P. (2001). Emerging themes in lipid rafts and caveolae. *Cell*, 106(4), 403.
- Gao, Z., & Schwartz, L. M. (2005). Identification and analysis of hic-5/ARA55 isoforms: Implications for integrin signaling and steroid hormone action. *FEBS Letters*, 579(25), 5651-5657.
- Gao, Z. L., Deblis, R., Glenn, H., & Schwartz, L. M. (2007). Differential roles of HIC-5 isoforms in the regulation of cell death and myotube formation during myogenesis. *Experimental Cell Research*, 313(19), 4000-4014.
- Gerace, L., & Blobel, G. (1980). The nuclear envelope lamina is reversibly depolymerized during mitosis. *Cell*, 19(1), 277.
- Ginn-Pease, M. E., & Whisler, R. L. (1998). Redox signals and NF- κ B activation in T cells. *Free Radical Biology and Medicine*, 25(3), 346-361.
- Goldman, R. D., Gruenbaum, Y., Moir, R. D., Shumaker, D. K., & Spann, T. P. (2002). Nuclear lamins: Building blocks of nuclear architecture. *Genes & Development*, 16(5), 533-547.
- Guignandon, A., Boutahar, N., Rattner, A., Vico, L., & Lafage-Proust, M. H. (2006). Cyclic strain promotes shuttling of PYK2/Hic-5 complex from focal contacts in osteoblast-like cells. *Biochemical and Biophysical Research Communications*, 343(2), 407-414.
- Haghighi, K., Kolokathis, F., Gramolini, A. O., Waggoner, J. R., Pater, L., Lynch, R. A., Dorn II, G. W. (2006). A mutation in the human phospholamban gene, deleting arginine 14, results in lethal, hereditary cardiomyopathy. *Proceedings of the National Academy of Sciences of the United States of America*, 103(5), 1388-1393.
- Halayko, A. J., Tran, T., & Gosens, R. (2008). Phenotype and functional plasticity of airway smooth muscle role of caveolae and caveolins. *Proceedings of the American Thoracic Society*, 5(1), 80-88.

- Heald, R., & McKeon, F. (1990). Mutations of phosphorylation sites in lamin A that prevent nuclear lamina disassembly in mitosis. *Cell*, *61*(4), 579-589.
- Heessen, S., & Fornerod, M. (2007). The inner nuclear envelope as a transcription factor resting place. *EMBO Reports*, *8*(10), 914-919.
- Helbling-Leclerc, A., Bonne, G., & Schwartz, K. (2002). Emery-dreifuss muscular dystrophy. *European Journal of Human Genetics: EJHG*, *10*(3), 157.
- Hu, Y., Cascone, P. J., Cheng, L., Sun, D., Nambu, J. R., & Schwartz, L. M. (1999). Lepidopteran DALP, and its mammalian orthologue HIC-5, function as negative regulators of muscle differentiation. *Proceedings of the National Academy of Sciences*, *96*(18), 10218-10223.
- Ishino, K., Kaneyama, J. K., Shibamura, M., & Nose, K. (2000). Specific decrease in the level of Hic-5, a focal adhesion protein, during immortalization of mouse embryonic fibroblasts, and its association with focal adhesion kinase. *Journal of Cellular Biochemistry*, *76*(3), 411-419.
- Jaalouk, D. E., & Lammerding, J. (2009). Mechanotransduction gone awry. *Nature Reviews Molecular Cell Biology*, *10*(1), 63-73.
- Je, H. D., Gallant, C., Leavis, P. C., & Morgan, K. G. (2004). Caveolin-1 regulates contractility in differentiated vascular smooth muscle. *American Journal of Physiology-Heart and Circulatory Physiology*, *286*(1), H91-H98.
- Kawamura, S., Miyamoto, S., & Brown, J. H. (2003). Initiation and transduction of stretch-induced RhoA and Rac1 activation through caveolae: Cytoskeletal regulation of ERK translocation. *Science Signaling*, *278*(33), 31111.
- Kelley, J. B., Datta, S., Snow, C. J., Chatterjee, M., Ni, L., Spencer, A., Paschal, B. M. (2011). The defective nuclear lamina in hutchinson-gilford progeria syndrome disrupts the nucleocytoplasmic ran gradient and inhibits nuclear localization of Ubc9. *Molecular and Cellular Biology*, *31*(16), 3378-3395.
- Kim-Kaneyama, J., Suzuki, W., Ichikawa, K., Ohki, T., Kohno, Y., Sata, M., Shibamura, M. (2005). Uni-axial stretching regulates intracellular localization of hic-5 expressed in smooth-muscle cells in vivo. *Journal of Cell Science*, *118*(5), 937-949.
- Kim-Kaneyama, J., Takeda, N., Sasai, A., Miyazaki, A., Sata, M., Hirabayashi, T., Nose, K. (2011). Hic-5 deficiency enhances mechanosensitive apoptosis and modulates vascular remodeling. *Journal of Molecular and Cellular Cardiology*, *50*(1), 77-86.
- Kozera, L., White, E., & Calaghan, S. (2009). Caveolae act as membrane reserves which limit mechanosensitive ICl, swell channel activation during swelling in the rat ventricular myocyte. *PLoS One*, *4*(12), e8312.

- Lammerding, J., Schulze, P. C., Takahashi, T., Kozlov, S., Sullivan, T., Kamm, R. D. Lee, R. T. (2004). Lamin A/C deficiency causes defective nuclear mechanics and mechanotransduction. *Journal of Clinical Investigation*, 113(3), 370-378.
- Lander, H. M. (1997). An essential role for free radicals and derived species in signal transduction. *The FASEB Journal*, 11(2), 118-124.
- Lee, H., Park, D. S., Razani, B., Russell, R. G., Pestell, R. G., & Lisanti, M. P. (2002). Caveolin-1 mutations (P132L and null) and the pathogenesis of breast cancer: caveolin-1 (P132L) behaves in a dominant-negative manner and caveolin-1 (-/-) null mice show mammary epithelial cell hyperplasia. *The American journal of pathology*, 161(4), 1357-1369.
- Lombardi, M. L., & Lammerding, J. (2011). Keeping the LINC: the importance of nucleocytoskeletal coupling in intracellular force transmission and cellular function. *Biochemical Society Transactions*, 39(6), 1729.
- Machiels, B. M., Zorenc, A. H. G., Endert, J. M., Kuijpers, H. J. H., van Eys, G. J. J. M., Ramaekers, F. C. S., & Broers, J. L. V. (1996). An alternative splicing product of the lamin A/C gene lacks exon 10. *Journal of Biological Chemistry*, 271(16), 9249-9253.
- Maraldi, N. M., Capanni, C., Cenni, V., Fini, M., & Lattanzi, G. (2011). Laminopathies and lamin-associated signaling pathways. *Journal of Cellular Biochemistry*, 112(4), 979-992.
- Méjat, A. (2010). LINC complexes in health and disease. *Nucleus*, 1(1), 40-52.
- Melcon, G., Kozlov, S., Cutler, D. A., Sullivan, T., Hernandez, L., Zhao, P., Rottman, J. N. (2006). Loss of emerin at the nuclear envelope disrupts the Rb1/E2F and MyoD pathways during muscle regeneration. *Human Molecular Genetics*, 15(4), 637-651.
- Milovanova, T., Chatterjee, S., Hawkins, B. J., Hong, N. K., Sorokina, E. M., DeBolt, K., Fisher, A. B. (2008). Caveolae are an essential component of the pathway for endothelial cell signaling associated with abrupt reduction of shear stress. *Biochimica Et Biophysica Acta (BBA)-Molecular Cell Research*, 1783(10), 1866-1875.
- Mounkes, L. C., Kozlov, S. V., Rottman, J. N., & Stewart, C. L. (2005). Expression of an LMNA-N195K variant of A-type lamins results in cardiac conduction defects and death in mice. *Human molecular genetics*, 14(15), 2167-2180.
- Muchir, A., Bonne, G., Van Der Kooi, A. J., Van Meegen, M., Baas, F., Bolhuis, P. A., . Schwartz, K. (2000). Identification of mutations in the gene encoding lamins A/C in autosomal dominant limb girdle muscular dystrophy with atrioventricular conduction disturbances (LGMD1B). *Human Molecular Genetics*, 9(9), 1453-1459.

- Nishiya, N., Tachibana, K., Shibamura, M., Mashimo, J. I., & Nose, K. (2001). Hic-5-reduced cell spreading on fibronectin: competitive effects between paxillin and Hic-5 through interaction with focal adhesion kinase. *Molecular and cellular biology*, *21*(16), 5332-5345.
- Nohe, A., Keating, E., Underhill, T. M., Knaus, P., & Petersen, N. O. (2005). Dynamics and interaction of caveolin-1 isoforms with BMP-receptors. *Journal of Cell Science*, *118*(3), 643-650.
- Novelli, G., Muchir, A., Sangiuolo, F., Helbling-Leclerc, A., D'Apice, M. R., Massart, C., Lauro, R. (2002). Mandibuloacral dysplasia is caused by a mutation in LMNA encoding lamin A/C. *The American Journal of Human Genetics*, *71*(2), 426-431.
- Nowlan, N. C., Prendergast, P. J., & Murphy, P. (2008). Identification of mechanosensitive genes during embryonic bone formation. *PLoS Computational Biology*, *4*(12), e1000250.
- Ohsawa, Y., Toko, H., Katsura, M., Morimoto, K., Yamada, H., Ichikawa, Y., Murakami, T., Ohkuma, S., Komuro, I., Sunada, Y. (2004). Overexpression of P104L mutant caveolin-3 in mice develops hypertrophic cardiomyopathy with enhanced contractility in association with increased endothelial nitric oxide synthase activity. *Human molecular genetics*, *13*(2), 151-157.
- Pagon, R. A., Bird, T. D., Dolan, C. R., Stephens, K., Adam, M. P., Bruno, C., Sotgia, F., Gazzerro, E., Minetti, C., & Lisanti, M. P. (2007). Caveolinopathies. *Gene reviews*, 2007.
- Parvari, R., & Levitas, A. (2012). The mutations associated with dilated cardiomyopathy. *Biochemistry Research International*, 2012
- Pekovic, V., Gibbs-Seymour, I., Markiewicz, E., Alzoughaibi, F., Benham, A. M., Edwards, R., Hutchison, C. J. (2011). Conserved cysteine residues in the mammalian lamin A tail are essential for cellular responses to ROS generation. *Aging Cell*, *10*(6), 1067-1079.
- Puckelwartz, M., & McNally, E. (2011). Emery-dreifuss muscular dystrophy. *Handbook of Clinical neurology*/edited by PJ Vinken and GW Bruyn, 101, 155.
- Puckelwartz, M. J., Depreux, F. F. S., & McNally, E. M. (2011). Gene expression, chromosome position and lamin A/C mutations. *Nucleus*, *2*(3), 162-167.
- Razani, B., Zhang, X. L., Bitzer, M., von Gersdorff, G., Böttinger, E. P., & Lisanti, M. P. (2001). Caveolin-1 regulates transforming growth factor (TGF)- β /SMAD signaling through an interaction with the TGF- β type I receptor. *Journal of Biological Chemistry*, *276*(9), 6727-6738.

- Shackleton, S., Lloyd, D. J., Jackson, S. N. J., Evans, R., Niermeijer, M. F., Singh, B. M., Durrington, P. N. (2000). LMNA, encoding lamin A/C, is mutated in partial lipodystrophy. *Nature Genetics*, 24(2), 153-156.
- Shibanuma, M., Iwabuchi, Y., & Nose, K. (2002). Possible involvement of hic-5, a focal adhesion protein, in the differentiation of C2C12 myoblasts. *Cell Structure and Function*, 27(1), 21-27.
- Shibanuma, M., Mashimo, J., Kuroki, T., & Nose, K. (1994). Characterization of the TGF beta 1-inducible hic-5 gene that encodes a putative novel zinc finger protein and its possible involvement in cellular senescence. *Journal of Biological Chemistry*, 269(43), 26767-26774
- Shibanuma, M., Mochizuki, E., Maniwa, R., Mashimo, J. I., Nishiya, N., Imai, S., Takano, T., Oshimura, M., Nose, K. (1997). Induction of senescence-like phenotypes by forced expression of hic-5, which encodes a novel LIM motif protein, in immortalized human fibroblasts. *Molecular and cellular biology*, 17(3), 1224-1235
- Shibanuma, M., & Nose, K. (1998). Forced expression of hic-5, a senescence-related gene, potentiates a differentiation process of RCT-1 cells induced by retinoic acid. *The international journal of biochemistry & cell biology*, 30(1), 39-45.
- Sieprath, T., Darwiche, R., & De Vos, W. H. (2012). Lamins as mediators of oxidative stress. *Biochemical and Biophysical Research Communications*
- Sinha, B., Köster, D., Ruez, R., Gonnord, P., Bastiani, M., Abankwa, D., Johannes, L. (2011). Cells respond to mechanical stress by rapid disassembly of caveolae. *Cell*, 144(3), 402-413.
- Spann, T. P., Moir, R. D., Goldman, A. E., Stick, R., & Goldman, R. D. (1997). Disruption of nuclear lamin organization alters the distribution of replication factors and inhibits DNA synthesis. *The Journal of Cell Biology*, 136(6), 1201-1212.
- Srinivasan, R., Forman, S., Quinlan, R. A., Ohanian, J., & Ohanian, V. (2008). Regulation of contractility by Hsp27 and hic-5 in rat mesenteric small arteries. *American Journal of Physiology-Heart and Circulatory Physiology*, 294(2), H961-H969.
- Stewart, C. L. (1993). Production of chimeras between embryonic stem cells and embryos. *Methods in enzymology*, 225, 823.
- Stick, R., Angres, B., Lehner, C. F., & Nigg, E. A. (1988). The fates of chicken nuclear lamin proteins during mitosis: Evidence for a reversible redistribution of lamin B2 between inner nuclear membrane and elements of the endoplasmic reticulum. *The Journal of Cell Biology*, 107(2), 397-406.
- Su, B., & Karin, M. (1996). Mitogen-activated protein kinase cascades and regulation of gene expression. *Current Opinion in Immunology*, 8(3), 402-411.

- Sullivan, T., Escalante-Alcalde, D., Bhatt, H., Anver, M., Bhat, N., Nagashima, K., Burke, B. (1999). Loss of A-type lamin expression compromises nuclear envelope integrity leading to muscular dystrophy. *The Journal of Cell Biology*, 147(5), 913-920.
- Sun, Y., Hu, G., Zhang, X., & Minshall, R. D. (2009). Phosphorylation of caveolin-1 regulates Oxidant-Induced pulmonary vascular permeability via paracellular and transcellular pathways. *Circulation Research*, 105(7), 676-685.
- Taylor, M. R. G., Slavov, D., Gajewski, A., Vlcek, S., Ku, L., Fain, P. R., Boucek, M. M. (2005). Thymopoietin (lamina-associated polypeptide 2) gene mutation associated with dilated cardiomyopathy. *Human Mutation*, 26(6), 566-574.
- Thorburn, J., Carlson, M., Mansour, S., Chien, K., Ahn, N., & Thorburn, A. (1995). Inhibition of a signaling pathway in cardiac muscle cells by active Mitogen-activated protein kinase kinase. *Molecular Biology of the Cell*, 6(11), 1479.
- Wang, P., Zhu, F., Tong, Z. Q., & Konstantopoulos, K. (2011). Response of chondrocytes to shear stress: Antagonistic effects of the binding partners toll-like receptor 4 and caveolin-1. *The FASEB Journal*, 25(10), 3401-3415.
- Wang, Y., Maciejewski, B. S., Drouillard, D., Santos, M., Hokenson, M. A., Hawwa, R. L., Sanchez-Esteban, J. (2010). A role for caveolin-1 in mechanotransduction of fetal type II epithelial cells. *American Journal of Physiology-Lung Cellular and Molecular Physiology*, 298(6), L775-L783.
- Woodman, S. E., Park, D. S., Cohen, A. W., Cheung, M. W. C., Chandra, M., Shirani, J., Christ, G. J. (2002). Caveolin-3 knock-out mice develop a progressive cardiomyopathy and show hyperactivation of the p42/44 MAPK cascade. *Journal of Biological Chemistry*, 277(41), 38988-38997.
- Worman, H. (2012). Nuclear lamins and laminopathies. *The Journal of Pathology*, 226(2), 316.
- Xie, L., Frank, P. G., Lisanti, M. P., & Sowa, G. (2010). Endothelial cells isolated from caveolin-2 knockout mice display higher proliferation rate and cell cycle progression relative to their wild-type counterparts. *American Journal of Physiology-Cell Physiology*, 298(3), C693-C701.
- Zwenger, M., Jaalouk, D. E., Lombardi, M. L., Isermann, P., Mauermann, M., Dialynas, G., Hermann, H., Wallrath, L.L., Lammerding, J. (2013). Myopathic lamin mutations impair nuclear stability in cells and tissue and disrupt nucleo-cytoskeletal coupling. *Human molecular genetics*

